



Earthquake Hazard and the Environmental Seismic Intensity (ESI) Scale

LEONELLO SERVA,¹ EUTIZIO VITTORI,² VALERIO COMERCI,² ELIANA ESPOSITO,³ LUCA GUERRIERI,²
ALESSANDRO MARIA MICHETTI,⁴ BAGHER MOHAMMADIOUN,⁵ GEORGIANNA C. MOHAMMADIOUN,⁵ SABINA PORFIDO,³ and
RUBEN E. TATEVOSSIAN⁶

Abstract—The main objective of this paper was to introduce the Environmental Seismic Intensity scale (ESI), a new scale developed and tested by an interdisciplinary group of scientists (geologists, geophysicists and seismologists) in the frame of the International Union for Quaternary Research (INQUA) activities, to the widest community of earth scientists and engineers dealing with seismic hazard assessment. This scale defines earthquake intensity by taking into consideration the occurrence, size and areal distribution of earthquake environmental effects (EEE), including surface faulting, tectonic uplift and subsidence, landslides, rock falls, liquefaction, ground collapse and tsunami waves. Indeed, EEEs can significantly improve the evaluation of seismic intensity, which still remains a critical parameter for a realistic seismic hazard assessment, allowing to compare historical and modern earthquakes. Moreover, as shown by recent moderate to large earthquakes, geological effects often cause severe damage⁷; therefore, their consideration in the earthquake risk scenario is crucial for all stakeholders, especially urban planners, geotechnical and structural engineers, hazard analysts, civil protection agencies and insurance companies. The paper describes background and construction principles of the scale and presents some case studies in different continents and tectonic settings to illustrate its relevant benefits. ESI is normally used together with traditional intensity scales, which, unfortunately, tend to saturate in the highest degrees. In this case and in unpopulated areas, ESI offers a unique way for assessing a reliable earthquake intensity. Finally, yet importantly, the ESI scale also provides a very convenient guideline for the survey of EEEs in earthquake-stricken areas, ensuring they are catalogued in a complete and homogeneous manner.

Key words: Earthquake geological effects, ESI, intensity scale, magnitude, seismic hazard assessment.

1. Introduction

Earthquake environmental effects (EEE) are all the effects, from geological to hydrological, physical and meteorological, that a seismic event can induce on the natural environment (MICHETTI *et al.* 2007). Among them, the coseismic geological effects are the most hazardous. They range from surface faulting, which can reach displacements of many meters and extend for hundreds of kilometers, to landslides, rock falls, liquefaction, ground collapse and many other consequences, including tsunamis.

Earthquake environmental effects are common features produced by moderate to large crustal earthquakes, in both their near and far fields. Always recorded and surveyed in recent events, very often they are remembered in historical accounts and conserved in the stratigraphic record as paleo-earthquake markers, the latter being the basis of paleoseismology (e.g., MCCALPIN 2009). Both surface deformation and faulting and shaking-related geological effects (e.g., liquefaction, landslides) not only leave permanent imprints in the environment, but can also severely impact man-made structures (e.g., HANCOX *et al.* 2002; HONEGGER *et al.* 2004; EERI 2008, 2011). Moreover, underwater fault ruptures and seismically triggered landslides can generate devastating tsunami waves (cf. WARD 2001; HARBITZ *et al.* 2006; TEN BRINK *et al.* 2009; OZAWA *et al.* 2011; SATAKE *et al.* 2013; and bibliography therein).

These phenomena represent significant sources of hazard, especially (but not exclusively) during large earthquakes, substantially contributing to the scenarios of destruction. Severe damage to buildings and infrastructure from surface faulting, landslides and liquefaction is commonly experienced during

¹ Via dei Dauni, 1, 00185 Rome, Italy.

² ISPRA, Istituto Superiore per la Protezione e la Ricerca Ambientale, Via Vitaliano Brancati, 48, 00144 Rome, Italy. E-mail: eutizio.vittori@isprambiente.it

³ IAMC-CNR, Calata Porta di Massa, 80133 Naples, Italy.

⁴ Dipartimento di Scienza e Alta Tecnologia, Università dell'Insubria, Via Valleggio, 11, 22100 Como, Italy.

⁵ Robin's Wood Consulting, 11612 Sheppard's Crossing Road, Whaleyville, MD 21872, USA.

⁶ Institute of the Physics of the Earth, Russian Academy of Sciences, B. Gruzinskaya 10, Moscow 123995, Russia.

moderate to strong seismic events (e.g., DOWRICK *et al.* 2008; MICHETTI *et al.* 2009; EBERHARD *et al.* 2010; HAYES *et al.* 2010; Lekkas 2010; EERI 2011; FRITZ *et al.* 2011; MORI *et al.* 2011; VITTORI *et al.* 2011; DI MANNA *et al.* 2013; HARP *et al.* 2013; MAVROULIS *et al.* 2013; PAVLIDES *et al.* 2013; SILVA *et al.* 2013; VALKANIOU *et al.* 2014). Our aim was to prove that seismic hazard assessment (SHA) would benefit from a comprehensive consideration of all earthquake-related effects, including environmental ones. Macroseismic intensity and its attenuation with distance are still considered key parameters for SHA and are used to generate shake maps for early warning and rapid response planning (e.g., SØRENSEN *et al.* 2009). According to the latter authors, ground motion attenuation in terms of macroseismic intensity allows to overcome some drawbacks of the commonly applied ground motion prediction equations (GMPEs), which are the limited number of recordings and the complex and not straightforward association of ground motion with damage.

A tool devised in the recent past (MICHETTI *et al.* 2007) to improve the intensity characterization is the Environmental Seismic Intensity (ESI) scale. It is a 12 degrees intensity scale (Table 1) solely based on EEEs, whose documentation has seen a considerable growth in the past decades. Several authors have made use of geological effects in their application of the Modified Mercalli (MM) intensity scale in the past, also influencing the advent of the ESI scale (e.g., DENGLER and MCPHERSON 1993; HANCOX *et al.* 2002). Many scientists all around the world have already applied the ESI scale in their account of recent and historical earthquake scenarios (see “Appendix”). The key contribution to SHA of the ESI scale is the improved intensity assessment, seen as the comprehensive parameter necessary to maintain the consistency between source parameters assessed for historical earthquakes and for the modern ones. The case of the 2012 Modena earthquake sequence clearly illustrated this point (e.g., GALLI *et al.* 2012; DI MANNA *et al.* 2013; GRAZIANI *et al.* 2015). Such consistency is pivotal for reliable magnitude/intensity relationships and the value of the seismic catalogue itself.

Therefore, based on several years of worldwide application in the field, in this paper (a) we introduce

the ESI scale to the community of earth scientists (geologists, geophysicists and seismologists) and civil engineers, as a survey instrument to better characterize a seismic event, also in terms of local effects and attenuation with distance, and (b) we provide insurers, civil protection agencies and administrators with an integrated tool to assess the potential damage deriving from geological effects during a future earthquake in an area, to be added to that directly associated to seismic shaking.

In the following, first a short summary of the evolution of earthquake intensity scales is given, also considering the impact of the advent of magnitude, followed by the background and rationale of the ESI scale. Then, three representative case studies target what are deemed to be the most crucial issues related to the application of the ESI scale, including: (a) the comparability of epicentral intensity assessed based on traditional macroseismic scales and on environmental effects, (b) the capability to measure paleo-earthquakes by means of the empirical relationships of rupture parameters (rupture length and displacement) with intensity and magnitude and (c) the assessment of epicentral intensity from the total area of secondary environmental effects and from the total rupture length (MICHETTI *et al.* 2007).

2. The Evolution of Intensity Scales and the Role of Environmental Effects

Over the past decades, a number of publications have dealt with the history of the intensity scales and the analysis of their relationships, from RICHTER (1958) and SHEBALIN (1975) to MUSSON *et al.* (2010). In the following, the focus is placed on how intensity was originally conceived and for what purposes. Before any standardized intensity scale had been conceived, a set of symbols were occasionally utilized for depicting different levels of damage of an earthquake, as in the map drawn by Matteo Greuter (Fig. 1) for the July 30, 1627, Gargano earthquake (in ZECCHI 2004). Something similar might already have appeared in Italy in the late 16th century, drawn by Gastaldi for the July 20, 1564, Nizza event, as cited in GIOFFREDO (1692), but this map, if it ever existed, is now lost. While this made it possible to compare

Table 1
The ESI scale

Degree	Primary effects	Secondary effects
I-II No perceptible environmental effects	Absent	Absent—extremely rare occurrence of small effects revealed only from instrumental observations, typically in the far field of strong earthquakes
III No perceptible environmental effects	Absent	Extremely rare occurrence of small variations in water level in wells and/or the flow-rate of springs, typically in the far field of strong earthquakes
IV No perceptible environmental effects	Absent	(a) Very few cases of fine cracking at locations where lithology (e.g., loose alluvial deposits, saturated soils) and/or morphology (slopes or ridge crests) are most prone to this phenomenon (b) Rare occurrence of small variations in water level in wells and/or the flow-rate of springs (c) Extremely rare occurrence of small variations of chemical-physical properties of water and turbidity of water in lakes, springs and wells, especially within large karst spring systems most prone to this phenomenon (d) Exceptionally, rocks may fall and small landslides may be (re)activated, along slopes where equilibrium is already very unstable, e.g., steep slopes and cuts, with loose or saturated soil (e) Extremely rare occurrence of karst vault collapses, which may result in the formation of sinkholes, where the water table is shallow within large karst spring systems (f) Very rare temporary sea level changes in the far field of strong earthquakes (g) Tree limbs may shake (a) A few cases of fine cracking at locations where lithology (e.g., loose alluvial deposits, saturated soils) and/or morphology (slopes or ridge crests) are most prone to this phenomenon (b) Extremely rare occurrence of significant variations in water level in wells and/or the flow-rate of springs (c) Rare occurrence of small variations of chemical-physical properties of water and turbidity of water in lakes, springs and wells (d) Rare small rock falls, rare rotational landslides and slump earth flows, along slopes where equilibrium is unstable, e.g., steep slopes, with loose or saturated soil (e) Extremely rare cases of liquefaction (sand boil), small in size and in areas most prone to this phenomenon (highly susceptible, recent, alluvial and coastal deposits, shallow water table) (f) Extremely rare occurrence of karst vault collapses, which may result in the formation of sinkholes, where the water table is shallow within large karst spring systems (g) Occurrence of landslides under sea (lake) level in coastal areas (h) Rare temporary sea level changes in the far field of strong earthquakes (i) Tree limbs may shake
V Marginal effects on the environment	Absent	

Table 1
continued

Degree	Primary effects	Secondary effects
VI Modest effects on the environment	Absent	<p>(a) Occasionally, thin, millimeter-wide, fractures are observed in loose alluvial deposits and/or saturated soils; along steep slopes or river banks they can be 1–2 cm wide. A few minor cracks develop in paved (asphalt/stone) roads</p> <p>(b) Rare occurrence of significant variations in water level in wells and/or the flow-rate of springs</p> <p>(c) Rare occurrence of variations of chemical-physical properties of water and turbidity of water in lakes, springs and wells</p> <p>(d) Rockfalls and landslides up to ca. 10 m³ can occur, especially where equilibrium is unstable, e.g., steep slopes and cuts, with loose/saturated soil, or weathered/fractured rocks. The area affected by them is usually less than 1 km²</p> <p>(e) Rare cases of liquefaction (sand boil), small in size and in areas most prone to this phenomenon (highly susceptible, recent, alluvial and coastal deposits, shallow water table)</p> <p>(f) Extremely rare occurrence of karst vault collapses, which may result in the formation of sinkholes</p> <p>(g) Occurrence of landslides under sea level in coastal areas</p> <p>(h) Occasionally, significant waves are generated in still waters</p> <p>(i) In wooded areas, trees shake; a very few unstable limbs may break and fall, also depending on species and state of health</p>
VII Appreciable effects on the environment	Primary effects observed very rarely. Limited surface faulting, with length of tens of meters and centimeter-wide offset, may occur associated with volcano-tectonic earthquakes	<p>(a) Fractures up to 5–10 cm wide are observed commonly in loose alluvial deposits and/or saturated soils; rarely in dry sand, sand-clay, and clay soil fractures up to 1 cm wide. Centimeter-wide cracks common in paved (asphalt or stone) roads</p> <p>(b) Rare occurrence of significant variations in water level in wells and/or the flow rate of springs. Very rarely, small springs may temporarily run dry or be activated</p> <p>(c) Quite common occurrence of variations of chemical-physical properties of water and turbidity of water in lakes, springs and wells</p> <p>(d) Scattered landslides occur in prone areas; where equilibrium is unstable (steep slopes of loose/saturated soils; rock falls on steep gorges, coastal cliffs) their size is sometimes significant (10³–10⁵ m³); in dry sand, sand-clay, and clay soil, the volumes are usually up to 100 m³. Ruptures, slides and falls may affect riverbanks and artificial embankments and excavations (e.g., road cuts, quarries) in loose sediment or weathered/fractured rock. The affected area is usually less than 10 km²</p> <p>(e) Rare cases of liquefaction, with sand boils up to 50 cm in diameter, in areas most prone to this phenomenon (highly susceptible, recent, alluvial and coastal deposits, shallow water table)</p> <p>(f) Possible collapse of karst vaults with the formation of sinkholes, even where the water table is deep</p> <p>(g) Occurrence of significant landslides under sea level in coastal areas</p> <p>(h) Waves may develop in still and running waters</p> <p>(i) In wooded areas, trees shake; several unstable branches may break and fall, also depending on species and state of health</p>

Table 1
continued

Degree	Primary effects	Secondary effects
VIII	Considerable effects on the environment	Primary effects observed rarely. Ground ruptures (surface faulting) may develop, up to several hundred meters long, with offsets generally smaller than 5 cm, particularly for very shallow focus earthquakes, such as volcano-tectonic events. Tectonic subsidence or uplift of the ground surface with maximum values in the order of a few centimeters may occur
		<p>(a) Fractures up to 25–50 cm wide are commonly observed in loose alluvial deposits and/or saturated soils; in rare cases fractures up to 1 cm can be observed in competent dry rocks. Decimeter-wide cracks common in paved (asphalt or stone) roads, as well as small pressure undulations</p> <p>(b) Springs can change, generally temporarily, their flow-rate and/or elevation of outcrop. Some small springs may even run dry. Variations in water level are observed in wells</p> <p>(c) Water temperature often changes in springs and/or wells. Water in lakes and rivers frequently becomes muddy, as well as in springs</p> <p>(d) Small to moderate (10^2–10^5 m³) landslides widespread in prone areas; rarely they can occur also on gentle slopes; where equilibrium is unstable (steep slopes of loose/saturated soils; rock falls on steep gorges, coastal cliffs) their size is sometimes large (10^5–10^6 m³). Landslides can occasionally dam narrow valleys causing temporary or even permanent lakes. Ruptures, slides and falls affect riverbanks and artificial embankments and excavations (e.g., road cuts, quarries) in loose sediment or weathered/fractured rock. The affected area is usually less than 100 km²</p> <p>(e) Liquefaction may be frequent in the epicentral area, depending on local conditions; sand boils up to ca. 1 m in diameter; apparent water fountains in still waters; localized lateral spreading and settlements (subsidence up to ca. 30 cm), with fissuring parallel to waterfront areas (river banks, lakes, canals, seashores)</p> <p>(f) Karst vaults may collapse, forming sinkholes</p> <p>(g) Frequent occurrence of landslides under the sea level in coastal areas</p> <p>(h) Significant waves develop in still and running waters</p> <p>(i) Trees shake vigorously, some branches or rarely even tree-trunks in very unstable equilibrium may break and fall</p> <p>(j) In dry areas, dust clouds may rise from the ground in the epicentral area</p>

Table 1
continued

Degree	Primary effects	Secondary effects
IX Natural effects leave significant and permanent traces	Primary effects observed commonly. Ground ruptures (surface faulting) develop, up to a few km long, with offsets generally smaller than 10–20 cm. Tectonic subsidence or uplift of the ground surface with maximum values in the order of a few decimeters may occur	<p>(a) Fractures up to 50–100 cm wide are commonly observed in loose alluvial deposits and/or saturated soils; in competent rocks they can reach up to 10 cm. Significant cracks common in paved (asphalt or stone) roads, as well as small pressure undulations</p> <p>(b) Springs can change their flow-rate and/or elevation of outcrop to a considerable extent. Some small springs may even run dry. Variations in water level are observed in wells</p> <p>(c) Water temperature often changes in springs and/or wells. Water in lakes and rivers frequently become muddy</p> <p>(d) Landsliding widespread in prone areas, also on gentle slopes; where equilibrium is unstable (steep slopes of loose/saturated soils; rock falls on steep gorges, coastal cliffs) their size is frequently large (10^5 m^3), sometimes very large (10^6–10^7 m^3 or $>$). Landslides can dam narrow valleys causing temporary or even permanent lakes. Riverbanks, artificial embankments and excavations (e.g., road cuts, quarries) frequently collapse. The affected area is usually less than 1000 km^2</p> <p>(e) Liquefaction and water upsurge are frequent; sand boils up to 3 m in diameter; apparent water fountains in still waters; frequent lateral spreading and settlements (subsidence of more than ca. 30 cm), with fissuring parallel to waterfront areas (river banks, lakes, canals, seashores)</p> <p>(f) Karst vaults of relevant size collapse, forming sinkholes</p> <p>(g) Frequent large landslides under the sea level in coastal areas</p> <p>(h) Large waves develop in still and running waters. Small tsunamis may reach the coastal areas with tidal waves up to 50–100 cm high</p> <p>(i) Trees shake vigorously; branches or even tree-trunks in unstable equilibrium frequently break and fall</p> <p>(j) In dry areas dust clouds may rise from the ground</p> <p>(k) In the epicentral area, small stones may jump out of the ground, leaving typical imprints in soft soil</p>

Table 1
continued

Degree	Primary effects	Secondary effects
X Environmental effects become dominant	<p>Primary ruptures become leading. Ground ruptures (surface faulting) can extend for several tens of km, with offsets reaching 50–100 cm and more (up to ca. 1–2 m in case of reverse faulting and 3–4 m for normal faulting). Gravity grabens and elongated depressions develop; for very shallow focus earthquakes, such as volcano-tectonic events, rupture lengths might be much lower. Tectonic subsidence or uplift of the ground surface with maximum values in the order of few meters may occur</p>	<p>(a) <i>Large landslides and rock-falls ($>10^5-10^7$ m³ or $>$) are frequent, practically regardless of equilibrium state of the slopes, causing temporary or permanent barrier lakes. River banks, artificial embankments and sides of excavations typically collapse. Levees and earth dams may even incur serious damage. The landslide-affected area is usually up to 5000 km²</i></p> <p>(b) Many springs significantly change their flow-rate and/or elevation of outcrop. Some may run dry or disappear, generally temporarily. Variations in water level are observed in wells</p> <p>(c) Water temperature often changes in springs and/or wells. Water in lakes and rivers frequently becomes muddy</p> <p>(d) <i>Open ground cracks up to more than 1 m wide are frequent, mainly in loose alluvial deposits and/or saturated soils; in competent rocks opening reaches several decimeters. Wide cracks develop in paved (asphalt or stone) roads, as well as pressure undulations zones; sand volcanoes even more than 6 m in diameter; vertical subsidence even >1 m; large and long fissures due to lateral spreading are common</i></p> <p>(f) Large karst vaults collapse, forming great sinkholes</p> <p>(g) Frequent large landslides under the sea level in coastal areas</p> <p>(h) <i>Large waves develop in still and running waters and crash violently into the shores. Running (rivers, canals) and still (lakes) waters may overflow from their beds. Tsunamis reach the coastal areas, with tidal waves up to a few meters high</i></p> <p>(i) Trees shake vigorously; branches or even tree-trunks very frequently break and fall, if already in unstable equilibrium</p> <p>(j) In dry areas, dust clouds may rise from the ground</p> <p>(k) <i>Stones, even if well anchored in the soil, may jump out of the ground, leaving typical imprints in soft soil</i></p>

Table 1
continued

Degree	Primary effects	Secondary effects
XI Environmental effects become essential for intensity assessment	Primary surface faulting can extend for several tens of km up to more than 100 km, accompanied by offsets reaching several meters. Gravity graben, elongated depressions and pressure ridges develop. Drainage lines can be seriously offset. Tectonic subsidence or uplift of the ground surface with maximum values in the order of many meters may occur	<p>(a) <i>Large landslides and rock-falls ($>10^5-10^6 \text{ m}^3$) are frequent, practically regardless of equilibrium state of the slopes, causing many temporary or permanent barrier lakes. River banks, artificial embankments and sides of excavations typically collapse. Levees and earth dams incur serious damage. Significant landslides can occur at 200–300 km distance from the epicenter. Primary and secondary environmental effects can be observed over territory as large as 10,000 km²</i></p> <p>(b) Many springs significantly change their flow-rate and/or elevation of outcrop. Frequently, they may run dry or disappear altogether. Variations in water level are observed in wells</p> <p>(c) Water temperature often changes in springs and/or wells. Water in lakes and rivers frequently becomes muddy</p> <p>(d) <i>Open ground cracks up to several meters wide are very frequent, mainly in loose alluvial deposits and/or saturated soils. In competent rocks they can reach 1 m. Very wide cracks develop in paved (asphalt or stone) roads, as well as large pressure undulations</i></p> <p>(e) <i>Liquefaction changes the aspect of extensive zones of lowland, determining vertical subsidence possibly exceeding several meters, numerous large sand volcanoes and severe lateral spreading features</i></p> <p>(f) Very large karst vaults collapse, forming sinkholes</p> <p>(g) Frequent large landslides under the sea level in coastal areas</p> <p>(h) <i>Large waves develop in still and running water and crash violently into the shores. Running (rivers, canals) and still (lakes) waters may overflow from their beds. Tsunamis reach the coastal areas with tidal waves up to many meters high</i></p> <p>(i) <i>Trees shake vigorously; many tree branches break and several whole trees are uprooted and fall</i></p> <p>(j) In dry areas dust clouds may arise from the ground</p> <p>(k) <i>Stones and small boulders, even if well anchored in the soil, may jump out of the ground leaving typical imprints in soft soil</i></p>

Table 1
continued

Degree	Primary effects	Secondary effects
XII	<p>Environmental effects are now the only tool enabling intensity to be assessed</p> <p>Primary surface faulting can extend for several hundreds of km up to 1000 km, accompanied by offsets reaching several tens of meters. Gravity graben, elongated depressions and pressure ridges develop. Drainage lines can be seriously offset. Landscape and geomorphological changes induced by primary effects can attain extraordinary extent and size (typical examples are the uplift or subsidence of coastlines by several meters, appearance or disappearance from sight of significant landscape elements, rivers changing course, origination of waterfalls, formation or disappearance of lakes)</p>	<p>(a) <i>Large landslides and rock-falls ($>10^5-10^6 \text{ m}^3$) are frequent, practically regardless of equilibrium state of the slopes, causing many temporary or permanent barrier lakes. River banks, artificial embankments, and sides of excavations typically collapse. Levees and earth dams incur serious damage. Significant landslides can occur at more than 200–300 km distance from the epicenter. Primary and secondary environmental effects can be observed over territory larger than 50,000 km²</i></p> <p>(b) Many springs significantly change their flow-rate and/or elevation of outcrop. Frequently, they may run dry or disappear altogether. Variations in water level are observed in wells.</p> <p>(c) Water temperature often changes in springs and/or wells. Water in lakes and rivers frequently becomes muddy</p> <p>(d) <i>Ground open cracks are very frequent, up to 1 m or wider in the bedrock, up to more than 10 m wide in loose alluvial deposits and/or saturated soils. These may extend up to several kilometers in length</i></p> <p>(e) <i>Liquefaction occurs over large areas and changes the morphology of extensive flat zones, determining vertical subsidence exceeding several meters, widespread large sand volcanoes and extensive severe lateral spreading features</i></p> <p>(f) Very large karst vaults collapse, forming sinkholes</p> <p>(g) Frequent very large landslides under the sea level in coastal areas</p> <p>(h) <i>Large waves develop in still and running water and crash violently into the shores. Running (rivers, canals) and still (lakes) waters overflow from their beds; watercourses change the direction of flow. Tsunamis reach the coastal areas with tidal waves up to tens of meters high</i></p> <p>(i) Trees shake vigorously; many tree branches break and many whole trees are uprooted and fall</p> <p>(j) In dry areas dust clouds may arise from the ground</p> <p>(k) <i>Even large boulders may jump out of the ground leaving typical imprints in soft soil</i></p>

Definitions in italics indicate the most diagnostic effects for each intensity degree

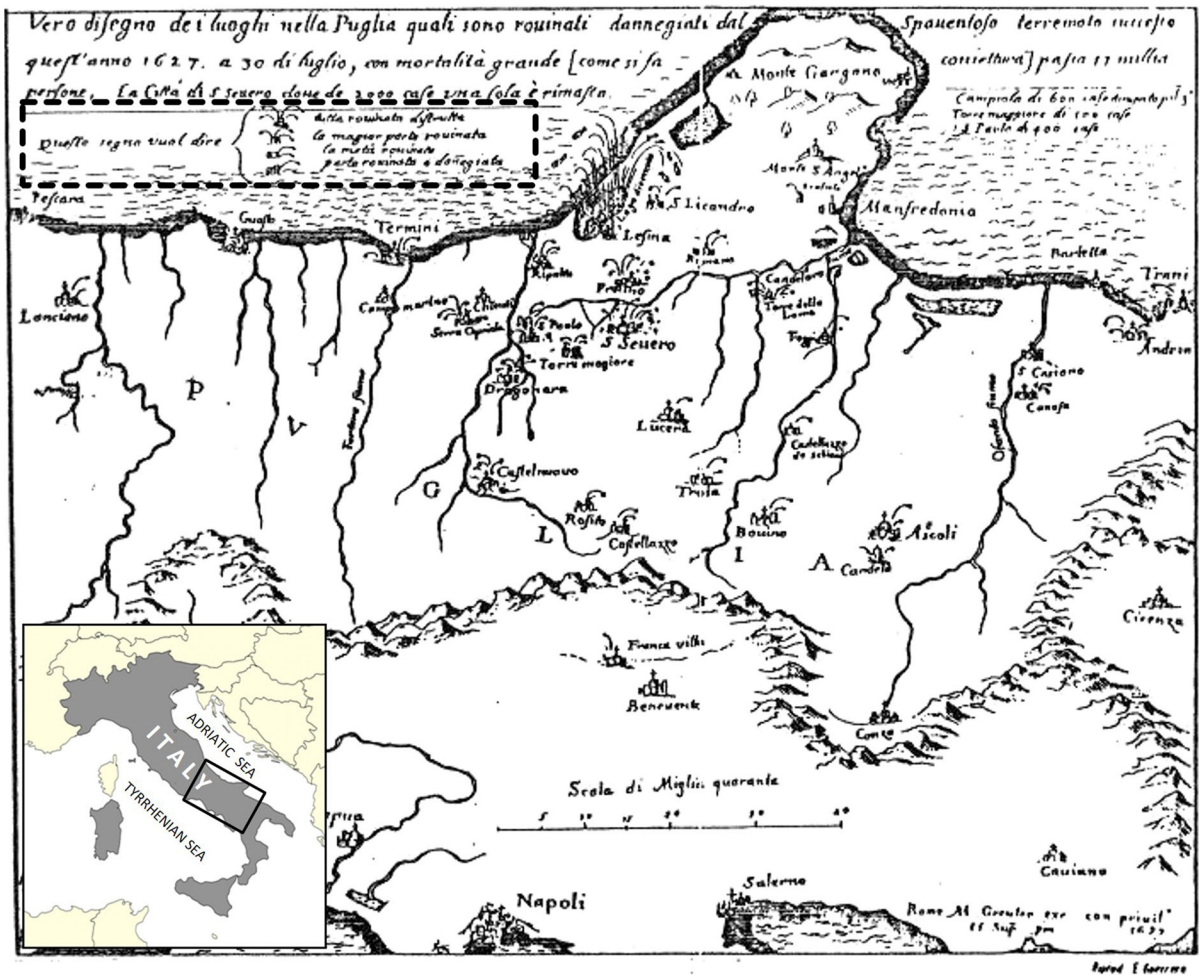


Figure 1

Matteo Greuter, Roma, 1627: distribution of damage caused by the July 30, 1627, Gargano earthquake in southern Italy; the stippled box encloses the map legend: *symbols* classify damage as completely destroyed, in large part destroyed, about half ruined, only partially ruined or damaged

damage caused by a given earthquake at different sites, it did not allow comparison among different earthquakes.

A number of strong events since the seventeenth century in many regions of Europe gradually increased the awareness that measuring and comparing earthquake effects was necessary, requiring a detailed documentation through a proper standardized procedure. A logical approach appeared to be the use of all the observable effects and consequences of an earthquake to represent its *size*. By the end of the nineteenth and in the early twentieth century, several intensity scales were conceived that divided the

whole range of seismic effects into characteristic sets commonly defined as degrees, now generally 10 to 12 in number. Their basic purpose was the same: to assess the size (strength) of earthquakes based on their effects on three different classes of targets: (1) domestic objects and human perception, (2) man-made engineered structures and infrastructures and (3) geological/natural environment.

Intensity scales had a threefold purpose: (1) to document the whole set of phenomena due to the earthquake; (2) to define a level of structural/environmental *damage* (I_i) in all the localities where it was felt, based on direct observation or deduced

from historical accounts; (3) to compare different earthquakes, based on the size of the observed effects and extent areas of similar levels of structural/environmental damage. The latter implies the possibility to classify earthquakes according to their epicentral intensity (I_0), i.e., the intensity within the epicentral area where the strongest effects usually take place. For example, when MUSHKETOV (1890), after a reconnaissance mission in the epicentral area of the May 28, 1887, Verny earthquake, wrote, “the earthquake strength was at least X degrees on the Rossi-Forel scale,” he meant the strength of the Verny earthquake as a natural phenomenon (see Fig. 2, where the area of maximum environmental effects is outlined). In fact, the environmental effects observed in the mountains were described in an extensive chapter, supported by drawings and photographs and used in earthquake strength assessment, on a par with damage incurred in towns and villages. Thus, in the earlier applications of the intensity scales the environmental effects were taken into account not differently from the effects on humans and manmade structures. See for example their wide use in the Mercalli–Cancani–Sieberg scale (MCS) or in the several versions and variants of the Modified Mercalli scale (e.g., DOWRICK *et al.* 2008; COMERCI 2013).

The advent of the earthquake magnitude scale (RICHTER 1935) greatly influenced the subsequent development of the intensity concept. Magnitude was deemed a more objective parameter, because it relates the instrumentally recorded ground displacement to its distance from the epicenter. Since then, a number of studies have appeared relating intensity to magnitude, with the goal to estimate magnitudes for historical, pre-instrumental, earthquakes. Information on their effects was collected going back as far as possible in history, sometimes over many centuries, as in Italy, Greece, Japan and China. The set of empirical relationships among intensity, source depth and magnitude, known as macroseismic field equations, takes a variety of forms. Some equations link I_0 directly to magnitude; others use generalized information on macroseismic effects in the form of isoseismals and solve the equations to obtain magnitude and source depth from ratios of isoseismal radii (I_i), and yet others are based on felt-areas (e.g., SHEBALIN 1972; AMBRASEYS 1985).

What is stressed here is that more weight was placed on intensity distribution rather than on I_0 . The intensity distribution, however, depends on the availability of observations and is, therefore, biased towards populated areas. More stable magnitude assessments can be derived from isoseismals than from a single I_0 . When observations are obtained in a large number of localities, a poor intensity assessment in one of them has little or no impact on the average isoseismal radius, while an erroneous I_0 assessment significantly affects the magnitude estimate. Another reason is that for many earthquakes the epicentral intensity could not be accurately defined, mainly because the epicenter was in a remote place.

Another achievement of instrumental seismology that has dramatically affected the intensity concept is the measurement of strong ground motion by accelerometers. Ground motion is mainly responsible for the observed intensity at a site (away from the surface faulting zone) and significantly contributes to its understanding (e.g., PANZA *et al.* 1997; WALD *et al.* 1999). However, such recordings cannot compete with intensity observations in terms of density of information and only rarely are available at the epicenter. In Japan, intensity (JMA scale) is now estimated based on the very dense array of strong-motion instruments and *seismic intensity-meters* (accelerometers) deployed there (e.g., NISHIMAE 2004). In the US, the ShakeMap program of the US Geological Survey produces near real-time shaking intensity maps from ground motion recordings (<http://earthquake.usgs.gov/earthquakes/shakemap/>).

With time, the focus on the behavior of engineering structures under seismic load, based on the estimation of local damage levels, has grown steadily in importance, radically restricting the original meaning of the intensity as an earthquake sizing parameter. The European Macroseismic scale (EMS98: GRÜNTAL 1998) openly discourages the use of EEEs with the comment: “while variations in the vulnerability of manmade structures can be presented in a reasonably coherent yet robust manner, in the case of the effects on nature, most of these depend on complex, geomorphological and hydrological features which cannot easily be assessed by the observer, or at all”. In our view, the significant improvements made in recent decades on the knowledge of the environmental effects



Figure 2

Map of the effects of the Verny, 1887, earthquake in the Tien Shan range of central Asia (from MUSHKETOV 1890). The small ellipse encloses the area of maximum environmental effects, while the large ellipse indicates the area of considerable damage. Both contours appear on Mushketov's original map. Note that most of the environmental effects occurred in a mountainous zone located 15–20 km south of the nearest populated area (Verny, now Almaty, Kazakhstan)

instead allow them to be fully exploited to categorize earthquake size, i.e., assess epicentral intensity, which is the rationale of the Environmental Seismic Intensity scale described hereinafter.

3. Earthquake Environmental Effects and ESI Scale

The ESI scale has been conceived not only to supplement the existing macroseismic intensity

scales, but also to work alone when the other scales cannot be applied (e.g., vast uninhabited areas). The reference macroseismic scales for calibration have been the MM and Medvedev–Sponheur–Karnik (MSK) scales, but also the MCS scale, after adjusted to align with the other (see for example the comparison table of intensities in REITER 1990). The choice of these scales was motivated by the wealth of historical information (also on environmental effects) available from their application for

over a century to earthquakes in many regions worldwide and to historical events going back in time for at least a millennium. This, and the database of surface rupture parameters (e.g., WELLS and COPPERSMITH 1994; and analysis in STIRLING *et al.* 2013) of events for which intensity data could be retrieved, allowed the tuning of the EEEs in the different degrees, in terms of manifestation, dimensions and density.

The extensive list of earthquakes in Table 2 helps clarify the application range of the ESI scale and its added value to macroseismic scales. In fact, many earthquakes of moderate to strong magnitude are assigned in the literature a small, unrealistic I_0 , despite extensive surface faulting and large offsets, e.g., the I_0 of IX for the 2004, Sumatra, M 9.1 event. Table 2 emphasizes also how the epicentral intensity and location of historical earthquakes can be poorly constrained based only on damage, when epicenters are located in sparsely populated areas with few buildings, or when the structural damage saturates, as it is usually seen, at intensity X of the historically used XII degrees scales cited before (MCS, MM, MSK). In some cases, the rupture parameters are not measured directly, but inferred from geophysical or instrumental seismological data, as for several events in the database of WELLS and COPPERSMITH (1994). Some occurrences in the data base are likely erroneous, e.g., the 1976 Gazli earthquake: its epicentral area was in the desert, and the expedition of the Institute of Physics of the Earth of Moscow observed only secondary effects (e.g., HARTZELL 1980).

The intensity values in Table 2 are undeniably correct, because they refer to the strongest macroseismic effects observed. However, they are far from representing that comprehensive measure of the event necessary for comparing seismicity in space and time, especially prior to the instrumental era, which is the prime scope of epicentral intensity. This current tendency in intensity estimation affects the development of reliable intensity/magnitude relationships, which serves to make the seismic events comparable in those catalogues that extend back in time well before the instrumental period even including paleoseismic events. This is the case, for example, for the Mediterranean region, China, Japan, and the USA. In this perspective, seismic intensity remains a

fundamental gauging parameter, despite the availability of more objective parameters, such as magnitude. The intensity assessment of many historical earthquakes is being updated as new archive documents are discovered or sources reinterpreted. Sometimes, the newly inferred magnitudes have a strong impact on SHA. However, to maintain or even improve its essential role, intensity should take advantage of all information pertaining to earthquake effects, on both built and natural environments, also considering that some geological effects (especially faulting, liquefaction, landslides) conserve a much longer “memory” than those on the man-made structures. This provides a unique tool for comparing and mutually calibrating prehistoric (paleoseismic), historical and modern earthquake datasets. Like macroseismic estimates, the application of the ESI scale must also take into account local effects of soil amplification and preexisting highly unstable slopes that may lead to locally overestimate the intensity. EEEs can be found only where the geological and morphological conditions exist for their occurrence, with an uneven coverage of territory. These drawbacks, however, do not lessen the value of the overall picture, similarly to what happens in all macroseismic field reconstructions..

EEEs fall into two main categories: (1) *primary effects*, which are the surface expression of the seismogenic source (e.g., surface faulting), normally observed for crustal earthquakes above a given magnitude threshold, generally close to 6.0 according to available sets of data (e.g., WELLS and COPPERSMITH 1994; YEATS *et al.* 1997); (2) *secondary effects*, mostly dependent on the characteristics of seismic wave and morphologic, geologic, climatic and soil conditions (e.g., landslides, liquefaction effects, ground cracks, etc.).

A good example of the contribution of EEEs to hazard assessment and earthquake characterization is provided by the empirical relationships of (1) magnitude and faulting parameters, in particular maximum/average displacement, surface rupture length and rupture area (e.g., WELLS and COPPERSMITH 1994; PAVLIDES and CAPUTO 2004; STIRLING *et al.* 2013), (2) magnitude and landslide distance from epicenter (e.g., KEEFER 1984; RODRÍGUEZ *et al.* 1999; HANCOX *et al.* 2002; PORFIDO *et al.* 2002; DELGADO

Table 2
Some earthquakes with epicentral intensities differing by 2 or more degrees between MM and ESI scales (SRL surface rupture length, MD maximum displacement)

Country	Epicentral Area	Date	M	SRL (km)	MD (m)	I ₀ MM	I ₀ ESI	References
USA, California	Arroyo Salada	19.03.1954	M _s 6.2	15	0.5	VI	X	WELLS and COPPERSMITH (1994) and WANG and TAO (2003); http://www.ngdc.noaa.gov/hazard/earthqk.shtml (accessed 25/06/2015)
Mexico	San Miguel	09.02.1956	M _s 6.9	22	1.15	VI	X	AMBRASEYS (1969), WELLS and COPPERSMITH (1994), HIRABAYASHI <i>et al.</i> (1996)
USA, Alaska	Huslia	07.04.1958	M _s 7.3	64	1.35	VIII	X	BRAZEE and CLOUD (1960) and STOVER and COFFMAN (1993)
USA, Alaska	Prince William Sound	28.03.1964	M _w 9.2	500	7–20	X	XII	VON HAKE and CLOUD 1966, KANAMORI (1977), STOVER and COFFMAN 1993, ABE (1995) and ATWATER <i>et al.</i> (1995); http://www.ngdc.noaa.gov/hazard/earthqk.shtml (accessed 25/06/2015)
Congo	Toro	20.03.1966	M _w 6.8	40	2.5	VII	X	LOUPEKINE (1966), YEATS <i>et al.</i> (1997), MAYONGA and DURRHEIM (2009)
Russia	Tajikistan-Xinjiang border	11.08.1974	M _s 7.3	30	1.2	VII–VIII	X	NIKONOV <i>et al.</i> (1983), WELLS and COPPERSMITH (1994), STIRLING <i>et al.</i> (2002) and WANG and TAO (2003)
Guatemala	Motagua	04.02.1976	M _s 7.5	235	3.4	IX	XI	ESPINOSA (1976), WELLS and COPPERSMITH (1994) and PORFIDO <i>et al.</i> 2015
USA, California	Mammoth Lakes	27.05.1980	M _s 6.0	20	0.5	VI	X	WELLS and COPPERSMITH (1994) and YEATS <i>et al.</i> (1997); http://earthquake.usgs.gov/earthquakes/eqarchives/significant/sig_1980.php (accessed 25/06/2015)
Papua New Guinea	New Ireland, Rabaul	03.07.1985	M _s 7.2	48		VII	XI	WELLS and COPPERSMITH (1994) and WANG and TAO (2003); http://earthquake.usgs.gov/earthquakes/eqarchives/significant/sig_1985.php (accessed 25/06/2015); http://www.ngdc.noaa.gov/hazard/earthqk.shtml (accessed 25/06/2015)
USA, California	Kettleman Hills	04.08.1985	M _s 5.9	20		VI	X	WELLS and COPPERSMITH (1994) and WANG and TAO (2003); http://earthquake.usgs.gov/earthquakes/eqarchives/significant/sig_1985.php (accessed 25/06/2015)

Table 2
continued

Country	Epicentral Area	Date	M	SRL (km)	MD (m)	I ₀ MM	I ₀ ESI	References
Canada	Nahanni	05.10.1985	M _s 6.6	32		VI	X	WELLS and COPPERSMITH (1994) and WANG and TAO (2003); http://earthquake.usgs.gov/earthquakes/eqarchives/significant/sig_1985.php , http://www.ngdc.noaa.gov/hazard/earthqk.shtml (accessed 25/06/2015)
Philippines	Luzon	16.07.1990	M _s 7.8	120	6.2	IX	XI	WELLS and COPPERSMITH (1994) and EQE ENGINEERING (1990)
Kyrgyzstan	Susamyr	19.08.1992	M _s 7.4	80	2.7	IX	XI	GÓMEZ <i>et al.</i> (1997) and YEATS <i>et al.</i> (1997); http://www.ngdc.noaa.gov/hazard/earthqk.shtml (accessed 25/06/2015)
Philippines	Mindoro	14.11.1994	M _s 7.1	>15	3.0	VI*	X	YEATS <i>et al.</i> (1997); http://earthquake.usgs.gov/earthquakes/eqarchives/significant/sig_1994.php ; http://www.ngdc.noaa.gov/hazard/earthqk.shtml (accessed 25/06/2015)
Taiwan	Chi-Chi	20.09.1999	M _w 7.6	83	11.3	IX	XI	HSU <i>et al.</i> (2002), SOKOLOV and WALD (2002) and STIRLING <i>et al.</i> (2002)
Perù	Coast of Perù	23.06.2001	M _w 8.4	370 [^]	4.5	VIII	XI	KIKUCHI and YAMANAKA (2002), RUEGG <i>et al.</i> (2001) and TAVERA <i>et al.</i> (2002); http://earthquake.usgs.gov/earthquakes/eqarchives/significant/sig_2001.php (accessed 26/06/2015)
USA, Alaska	Denali National Park	03.11.2002	M _w 7.9	340	8.8	IX	XI	EBERHART-PHILLIPS <i>et al.</i> (2003), HÄUSSLER <i>et al.</i> (2004), MARTIROSYAN (2004) and HÄUSSLER (2009); http://www.aeic.alaska.edu/Seis/Denali_Fault_2002/ (accessed 26/06/2015), http://earthquake.usgs.gov/earthquakes/dyfi/events/ak/22614036/us (accessed 26/06/2015)
Mexico	Colima	22.01.2003	M _w 7.4	40	3.0	VIII	X	http://fisee.kenken.go.jp/special/20030122colima.htm (accessed 26/06/2015), http://earthquake.usgs.gov/earthquakes/eqarchives/year/2003/2003_01_22.php (accessed 26/06/2015)

Table 2
continued

Country	Epicentral Area	Date	M	SRL (km)	MD (m)	I_0 MM	I_0 ESI	References
Indonesia	Sumatra–Andaman Islands	26.12.2004	M_w 9.1	1300–1500	20.0	IX	XII	BILHAM <i>et al.</i> (2005), MARTIN (2005), BANERJEE <i>et al.</i> (2007) and CHLIEH <i>et al.</i> (2007); http://earthquake.usgs.gov/earthquakes/eqinthenews/2004/us2004slav/ (accessed 26/06/2015)

et al. 2013; COMERCI *et al.* 2013; ESPOSITO *et al.* 2013) and (3) magnitude and liquefaction distance from epicenter (GALLI 2000; CASTILLA and AUDEMARD 2007; and references therein). The aforementioned relationships, although largely empirical and characterized by considerable scattering, are widely applied in both deterministic and probabilistic SHA studies, especially (1). The same empirical analysis can be carried out based on intensity (see for example the graphs in MICHETTI *et al.* 2004), which is the basic approach of the ESI scale, where several other environmental effects are also taken into account statistically.

The importance of EEES as a tool to measure earthquake intensity was already outlined in the early 1990s, for example by DENGLER and MCPHERSON (1993) and SERVA (1994). An MMI-derived scale has been developed in New Zealand (HANCOX *et al.* 2002) that incorporates landsliding, liquefaction and other ground damage criteria, but excluding primary effects, regarded as a seismogenic effect unrelated to shaking and, therefore, neither to intensity.

The concept of an intensity scale exclusively based on environmental effects took form in the 1999 15th INQUA Congress, Durban. A first version of the scale was presented in 2003 (16th INQUA Congress, Reno, MICHETTI *et al.* 2004) and tested over a 4-year trial period using actual case studies worldwide. The ESI 2007 intensity scale, presented in the framework of the 2007 17th INQUA Congress in Cairns, Australia, has taken into account the results of these applications.

In the following, the basic structure of the ESI 2007 is discussed. The full text is given in Table 1 (Michetti *et al.* 2007) and is available on-line in several languages (http://www.isprambiente.gov.it/it/pubblicazioni/periodici-tecnici/memorie-descrittive-della-carta-geologica-ditalia/memdes_97.pdf).

In order to make the ESI 2007 scale more compatible with previous macroseismic scales, it maintains two different levels of EEE spatial generalization: *site* and *locality*.

Site corresponds to the place where a single EEE of a certain type was observed, such as a landslide or a ground crack. This is the level at which EEE descriptions have to be compiled. As these effects are strongly dependent not only on the severity of

shaking, but also on many other physical factors, it is only possible to assign an interval of probable intensity values to the effect observed at the site.

Locality is the place including one or more sites where the EEE occurred and presents a level of generalization to which intensity can be assigned. It is assumed that within the spatial frame of a locality, when EEE occurred in several sites, peculiar effects associated with the specific characteristics of each site are removed. Locality can refer to any place, whether populated or not. Since a natural “locality” can be anything from a river valley to a mountain slope or a large hill, it is difficult to assign a typical dimension to it, although it must be small enough to avoid comprising separate areas with significantly different site intensities, but large enough to include more than one site and consequently to be representative for an intensity assessment. Therefore, the definition of locality boundaries is a matter of expert judgment.

An analogue of locality in traditional macroseismic studies is a village or a medium-sized town, to which an intensity value can be assigned. Sometimes, intensities differing by one or even two degrees are found for the same town, commonly due to site effect conditions. In such a case, conservatively, the highest intensity is generally taken, if the scale of representation does not allow all values to be displayed. The site is an analogue of a single macroseismic object. For a single building, the degree of damage can be defined, but not a well-defined intensity value.

In the classical macroseismic intensity assessments, a statistical analysis of damage levels for different categories of structures (differentiation is based on their vulnerability) within the city or town provides the intensity of shaking at this locality. In contrast, expert judgement of EEEs at a given locality is used for the ESI scale. This evaluation concerns both the probable range of intensities observed as well as the accuracy of the estimates. By adopting the “locality-site” concept, a merging of environmental and macroseismic effects into a unified intensity scale might be almost straightforwardly achieved.

The EEE intensity field resulting from this process provides an additional portrait of the earthquake. A comparison with the “traditional” macroseismic fields of the same earthquake has shown so far a fairly good agreement, generally within one degree (see

references on its application listed in the “[Introduction](#)”). However, significant discrepancies in intensity assessments ($>$ one degree) must be accounted for with a dedicated analysis. They can result from: (a) a site amplification selectively affecting the human or natural environment to a greater extent (for example, topographic or soft sediment amplification effects), (b) an anomalously strong or light damage because of building type and/or quality. Moreover, although it has worked satisfactorily so far, the ESI scale is still a novel tool. Some fine-tuning might emerge as useful in the future, based on experience gained by its application to more cases.

Based on the ESI scale (Tables 1, 3), the size of the *epicentral area*, i.e., the area where the strongest effects are observed, as well as the total area affected by EEEs, allow I_0 to be estimated. The latter also scales with rupture parameters: surface rupture length (SRL) and maximum displacement (MD) that are also rather well correlated with magnitude. This is particularly useful for assessing the size of paleo-earthquakes, where proxies of intensity/magnitude data are extremely rare. Relationships between the total area of specific secondary effects (e.g., landslides or liquefactions) and I_0 , despite more complex, also make it possible to estimate the earthquake size (Table 1). In addition, recent studies confirm that factors such as the total number, size and density of landslides may provide a sound means of assessing the strength of shaking across an earthquake-affected area (HANCOX *et al.* 2002, 2014, and references therein).

However, there are instances where the instrumental and macroseismic epicenters are far apart; the typical example is the Mexico City earthquake in 1985, where an M8.1 subduction event caused its greatest damage more than 350 km away, in the soft lacustrine setting of Mexico City (e.g., CAMPILLO *et al.* 1989; CHAVEZ-GARCIA and BARD 1994). This is a particular case where the local amplifications (mostly liquefaction and ground compaction in Mexico City and sparse landslides over a wide region) have to be taken into proper consideration, together with other information, most likely leading to excluding the Mexico City data for assessing I_0 . The characteristics of the EEEs of many earthquakes worldwide, including the assessed ESI intensity, are reported in

Table 3

Ranges of surface faulting parameters and typical extents of total area for each intensity degree (SRL: surface rupture length, MD: maximum surface displacement or deformation, Total Area: area of occurrence of EEEs)

I_0 Intensity	Primary effects		Secondary effects
	SRL	MD	Total area (km ²)
IV	–	–	–
V	–	–	–
VI	–	–	–
VII	(*)	(*)	10
VIII	Some hundred meters	Centimeters	100
IX	1–10 km	5–40 cm	1000
X	10–60 km	40–300 cm	5000
XI	60–150 km	300–700 cm	10,000
XII	>150 km	>700 cm	>50,000

(*) Limited surface fault ruptures, tens to a few hundreds of meters long with offset of a few centimeters, may occur, more often associated with very shallow earthquakes, especially in volcanic areas

the EEE Catalogue, hosted by ISPRA in the framework of the INQUA TERPRO Focus Area on Paleoseismicity project “A global catalogue and mapping of Earthquake Environmental Effects” (<http://www.eeecatalog.sinanet.apat.it/terremoti>). The same data set is currently also accessible through the United Nations—International Atomic Energy Agency—International Seismic Safety Center (IAEA-ISSC) webpage ([issc.iaea.org](http://www.issc.iaea.org)).

4. Case Studies of Application of the ESI Scale

Many papers published so far illustrate the application of the ESI scale to recent, historical and paleo-earthquakes (cf. list of references in the “Introduction”). In the following, some recent and historical case studies, representative of different seismotectonic environments (location in Fig. 3), focus on some key questions. The first case study is an example of how regional and local factors affect earthquake size assessment. Then, the 1805 Italy earthquake is used to illustrate how the distribution of maximum secondary effects makes it possible to assess I_0 and to identify the seismogenic source. In a third example, the Denali 2002 earthquake serves to highlight the problem of epicentral intensity assessment, when the epicenter is far from populated areas.

4.1. Focusing on How Regional and Local Factors Affect Earthquake Size Assessment: the June 27, 1957, Muya (Baikal, Russia) Earthquake

Systematic studies of paleo-earthquakes started in the Baikal region in the early 1960s; the first regional catalogue of paleo-earthquakes was published in KONDORSKAYA and SHEBALIN (1982).

Baikal is a unique zone of active continental rifting. The almost pure normal faulting of published CMT-solutions (inset of Fig. 4) is in full agreement with this general geodynamic framework. However, the largest known earthquake in the region, the 1957 Muya earthquake ($M_{lh} = 7.6$, $M_S = 7.5$), demonstrates a much more complex faulting style, with a relevant strike-slip component found both in source modeling and in surface ruptures (Fig. 5). Surface ruptures associated with the earthquake were studied during several field investigations and summarized in reports and papers by KURUSHIN (1963), SOLONENKO (1965), SOLONENKO *et al.* (1966, 1985) and KURUSHIN and MEL'NIKOVA (2008) (Fig. 5). Figure 4 summarizes the macroseismic information, based on questionnaires collected in 1958 by the Institute of the Physics of the Earth, RAS and data from SOLONENKO *et al.* (1958). Noteworthy is the far-reaching extension of the felt area, over 700 km away from the surface faulting zone.

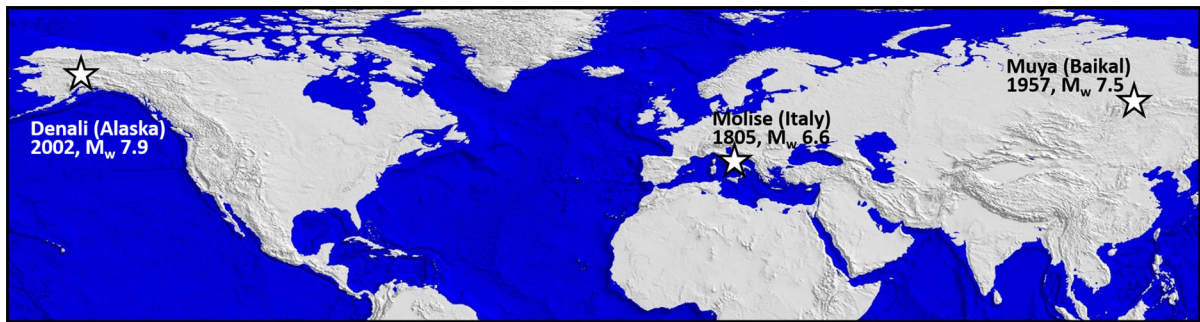


Figure 3
Location of earthquake case-studies discussed in this paper

According to the ESI scale, epicentral intensity can also be assessed based on the total length (SRL) and maximum displacement (MD) of the observed surface faulting. The surface ruptures of the Muya event occurred along three main WNW trending *en echelon* segments with partly lateral and normal slip components (Fig. 5). The reported 20–25 km of SRL corresponds to an epicentral ESI intensity X. The maximum offset (vertical) was 3.3 m, which, for normal faulting, is also in agreement with an intensity of at least X. Instead, since the villages nearest the surface rupture zone were 50 km away, the maximum observed macroseismic intensity was rather low compared to the magnitude of the event, not reaching VIII. Thus, if only macroseismic effects are considered for epicentral intensity assessment, I_0 would be underestimated by no less than two degrees.

The epicentral locations determined instrumentally differ from each other by more than 100 km (ISC 2012). The instrumental hypocenter depth varies from 10 (DOSER 1991) to 22 km (BALAKINA *et al.* 1972). TATEVOSSIAN *et al.* (2010) have assessed a depth around 20 km, applying the macroseismic field equation for Baikal region found in KONDORSKAYA and SHEBALIN (1982) for $M_{lh} = 7.6$ and a radius of felt shaking of 700 km (Fig. 4). The rather short surface faulting zone (20–25 km) is also supportive of the relatively deep source, common in the Baikal region (e.g., DÉVERCHÈRE *et al.* 2001). For the sake of comparison, the 2003 Altai earthquake ($M_s = 7.4$) was accompanied by 70 km of surface ruptures (SRL) (TATEVOSSIAN *et al.* 2009). According to WELLS and COPPERSMITH (1994), a 20–25 km SRL would

correspond to M_s 6.6, much lower than that measured (see, for example, TATEVOSSIAN 2011). The short SRL and large MD (maximum displacement) could also be representative of a source with high stress drop, a possible trait of the regional seismicity. Thus, the influence of regional tectonics and structural characteristics on the coseismic effects should also be considered in the paleoseismic evaluations.

4.2. Focusing on the Distribution of Maximum Secondary Effects to Assess I_0 and to Identify the Seismogenic Source: the July 26, 1805, Molise (Southern Italy) Earthquake

The 1805 Molise earthquake (Southern Italy) was characterized by a main shock (macroseismically derived magnitude $M_a = 6.6$) followed a few hours later by two important aftershocks. The epicentral zone was centered in the Bojano plain ($I_0 = X$ MCS; LOCATI *et al.* 2011), and an area of about 2000 km² was affected by MCS intensities $\geq VIII$. ESPOSITO *et al.* (1987) locate the macroseismic epicenter of the main shock (Figs. 6, 7) at Frosolone ($I_{max} = XI$ MCS). The epicenter of the second main shock was located at Morcone, some tens of kilometers to the southeast.

The historical accounts of the 1805 earthquake mention about one hundred seismically induced environmental effects, mostly in the near-field area, although some were reported as far away as 70 km from the epicenter (ESPOSITO *et al.* 1987; PORFIDO *et al.* 2002). The most relevant effects documented in contemporary sources are described in Table 4 and

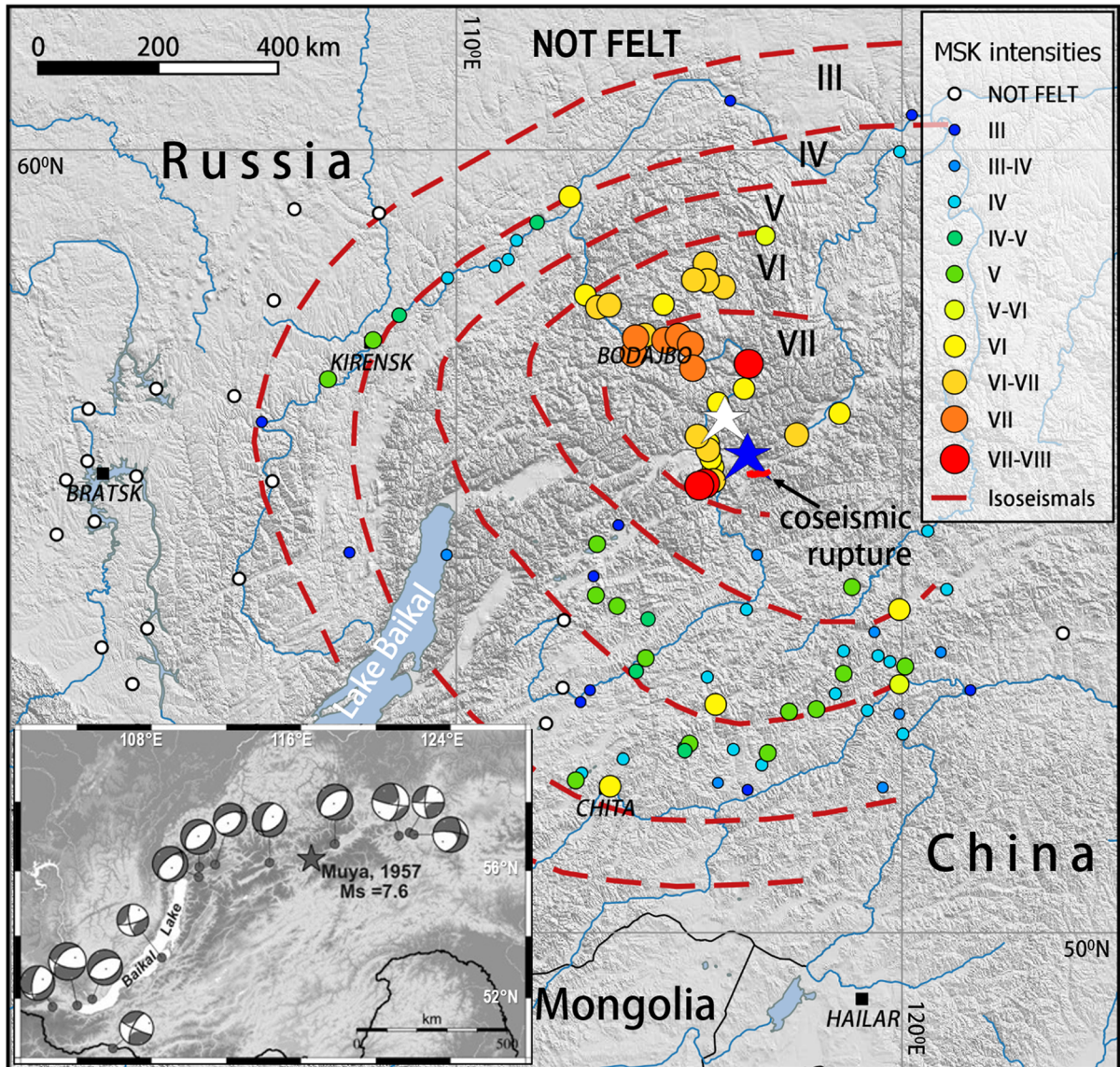


Figure 4

Approximate macroseismic (white star) and instrumental (blue star, according to VVEDENSKAYA and BALAKINA 1960) epicenters of the Muya, 1957, earthquake, and MSK intensities (degrees in Roman numerals). Inset in lower left: source mechanisms in the Baikal region for events with $M_0 \geq 10^{24}$ dyn cm ($M_w \geq 5.3$) (<http://www.globalcmt.org/CMTsearch.html>), showing a dominant extension in the Baikal rift grading into ca. east–west left-lateral slip eastward of the Muya region

mapped in Fig. 7. Among these, vertical ground displacements of about 1.5 m at Guardiaregia and Morcone are interpreted as primary effects. Along an antithetic fault, a long fracture reported between Pesche and Miranda and northeast of Castelpetroso may also be interpreted as evidence of surface faulting. This fact would indicate that the total rupture length was about 40 km, with maximum

displacements of about 1.5 m at Guardiaregia. Consequently, the ESI epicentral intensity is X.

The earthquake also triggered a number of secondary effects, notably, slope movements, hydrological anomalies and liquefaction. At least 26 mass movements (rock falls, topples, slumps, earth flows and slump earth flows) were recorded (ESPOSITO *et al.* 1987, 1998; PORFIDO *et al.* 2007; SERVA *et al.* 2007).

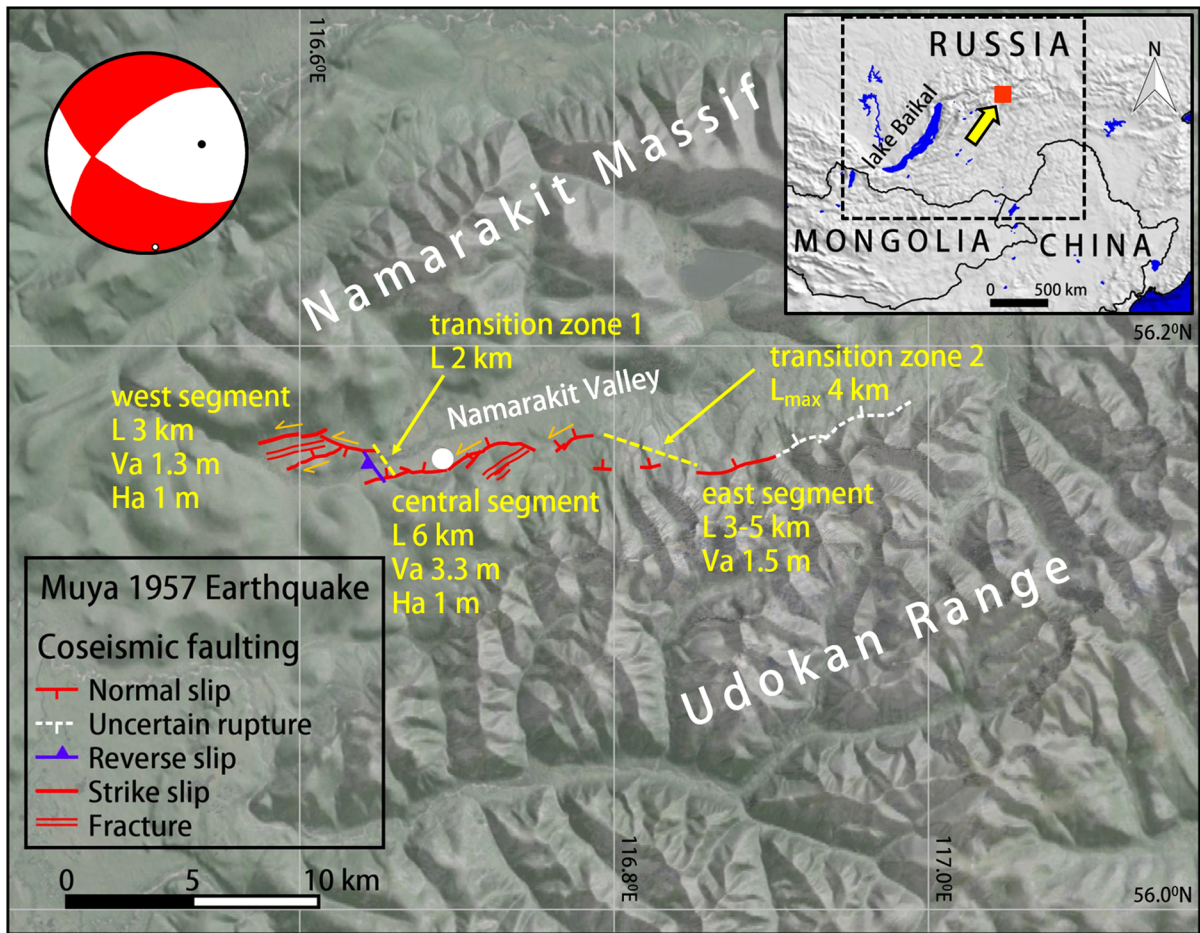


Figure 5

Surface faulting of the 1957 Muya earthquake; stippled in white is a doubtful portion of the coseismic rupture (L rupture length, V_a average vertical component of slip, H_a average horizontal component of slip). Orange arrows mark sections with substantial horizontal slip. Three main segments can be discerned, separated by transition zones. The focal mechanism shown, from VVEDENSKAYA and BALAKINA (1960), is very similar to the three subevents reconstructed by DOSER (1991). White dot is approximate location of top photograph in Fig. 11

In 29 localities, principally around Bojano (Biferno springs) and the Matese Massif, 48 hydrological anomalies were reported, mainly changes in water discharge from springs. Flow increases were observed in at least 16 springs, mainly SSW of the Matese Mountains. New springs also appeared, one of them at Bojano was active for about 2 months after the earthquake (ESPOSITO *et al.* 1987, 2001; Porfido *et al.* 2002). Only one clear case of liquefaction was reported at Cantalupo. Flames were also seen escaping from the supposed fault rupture at Morcone, likely burning methane from palustrine sediments. Furthermore, anomalous sea waves were observed in the gulfs of Naples and Gaeta (CAPUTO and FAITA

1984; ESPOSITO *et al.* 1987; TINTI and MARAMAI 1996; MARAMAI *et al.* 2014), the cause of which is unidentified, possibly submarine landslides or resonance effects.

The application of the ESI scale to secondary effects has allowed local intensity values between V and X to be assigned to about 50 municipalities (SERVA *et al.* 2007; Fig. 7). The total area of relevant ground effects (ESI local intensities \geq VII) amounts to about 5300 km². According to Table 3, the ESI epicentral intensity is X.

In conclusion, this case study shows that both primary and secondary effects, when properly taken into account, can serve for:

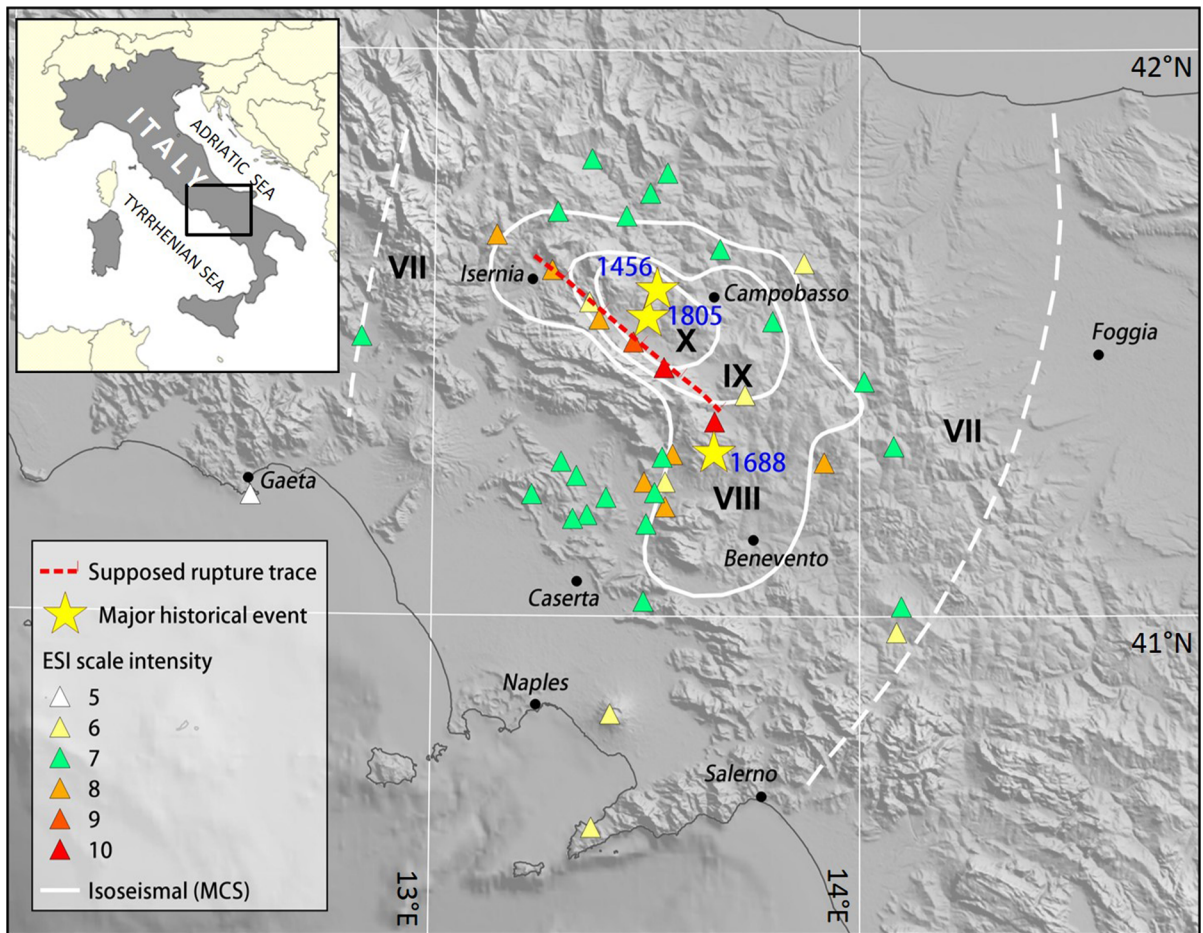


Figure 6

1805 Molise earthquake: comparison of MCS and ESI macroseismic intensity fields. *White lines* MCS isoseismals (MCS degrees in Roman numerals, after ESPOSITO *et al.* 1987). The highest intensity was seen at Frosolone, slightly west of the 1456 epicenter. ESI local intensities (*triangles*) are after SERVA *et al.* (2007). Only the epicenters of the three major historical earthquakes in the near area are shown. Likely, the 1456 and 1805 events occurred along the same fault

1. Intensity assessment: in fact, two independent applications of the ESI, from the total area of secondary effects and from SRL, have yielded the same $I_0 = X$. This result is also consistent with the independently assessed macroseismic intensity (MCS = X).
2. Identification of the seismogenic source: the scenario of secondary effects allows the seismogenic source to be located on the southwestern border of the Bojano basin, in good agreement with local evidence of surface faulting reported in historical documents at Morcone, Guardiaregia and Pesche (Table 4), confirmed by recent studies

(GUERRIERI *et al.* 1999; BLUMETTI *et al.* 2000; GALLI and GALADINI 2003).

4.3. Focusing on Epicentral Intensity Assessment, When the Epicenter is Far from Populated Areas: the November 3, 2002, Denali (Alaska) Earthquake

The 2002 Denali earthquake ($M_w = 7.9$) was the largest strike-slip earthquake in North America in more than 150 years (HANSEN and RATCHKOVSKI 2004; MARTIROSYAN 2004). The epicenter was located

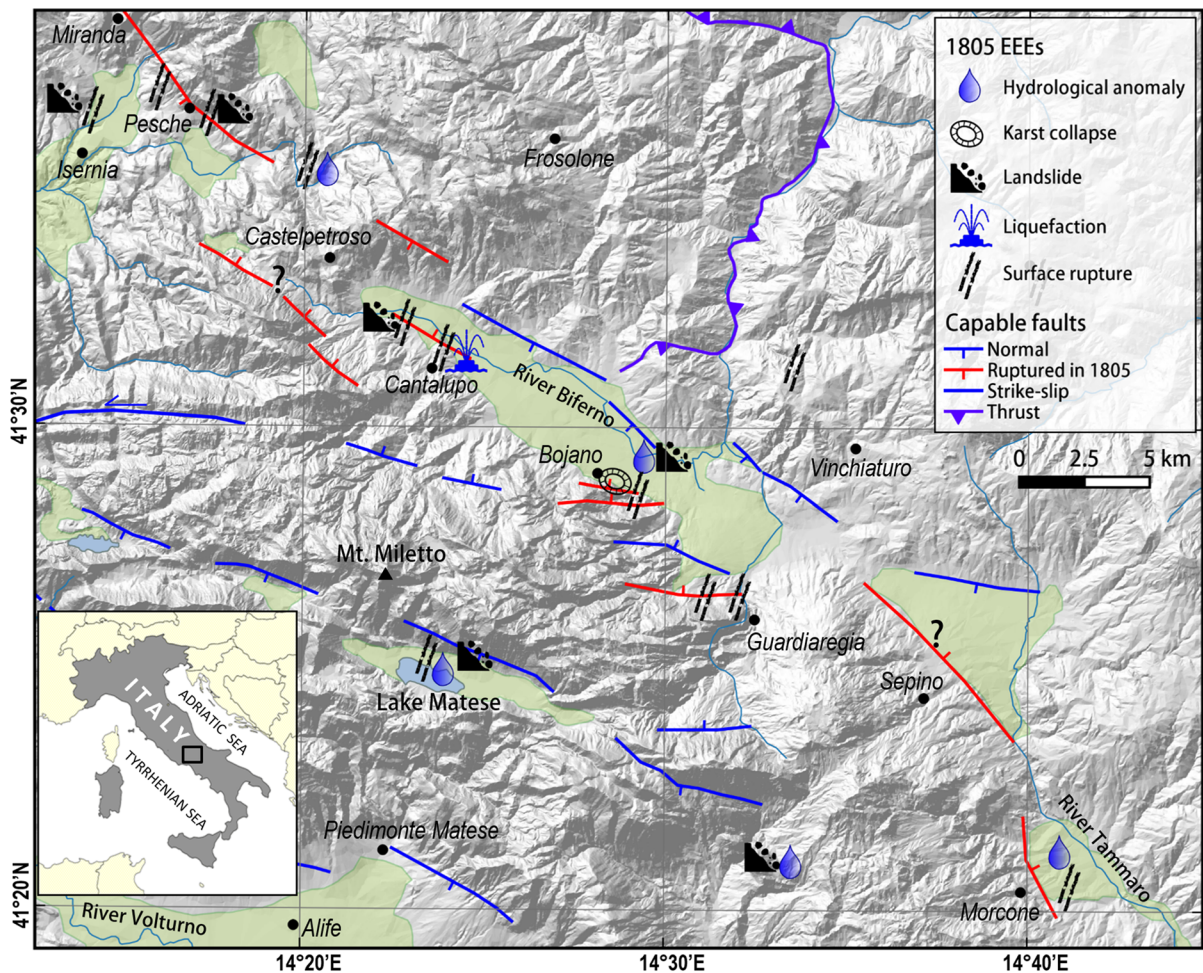


Figure 7

Distribution of the main geological effects reported for the 1805 Molise earthquake (data after PORFIDO *et al.* 2002). The Bojano fault system, running northwest–southeast, has controlled the Quaternary evolution of the Bojano and adjacent intermountain basins, marked in light green, the largest of them being Morcone and Sepino (? where rupture is doubtful)

135 km south of Fairbanks and 280 km north of Anchorage (Fig. 8). The total surface fault rupture length was about 330 km, running ca. east–west at its northwestern tip and then WNW–ESE; the maximum displacement was 8.8 m right-lateral, measured west of the Denali and Totschunda fault junction, and over 5 m reverse on the Susitna Glacier fault (EBERHART-PHILLIPS *et al.* 2003; AAGAARD *et al.* 2004; CRONE *et al.* 2004; FRANKEL 2004; HANSEN and RATCHKOVSKI 2004; HAEUSSLER 2009). Three sub-events were identified (EBERHART-PHILLIPS *et al.* 2003; FRANKEL 2004), and a total seismic moment equivalent to $M_w = 7.9$ was inferred from GPS data, also consistent with

that derived from InSAR data (WRIGHT *et al.* 2004). The first sub-event ($M_w = 7.2$), located near the instrumental epicenter, was associated with the rupture along the Susitna Glacier Fault. The second sub-event ($M_w = 7.3$) was 50–100 km east of the epicenter, where the surface offset of the Denali Fault reached over 6 m. It is noteworthy that, despite this, the Trans-Alaska Pipeline did not produce any oil spill, thanks to a technical solution devised after the experience of the 1964 Alaska earthquake (HONEGGER *et al.* 2004). The third sub-event had the largest seismic moment, equivalent to $M_w = 7.6$, and was located about 130–220 km east of the epicenter,

where the maximum surface offset of 8.8 m was measured (EBERHART-PHILLIPS *et al.* 2003; FRANKEL 2004).

The effects of rupture directivity are particularly remarkable for the Denali fault event. Ground shaking effects were reported as far away as almost 6000 km from the epicenter: for example, in Louisiana, seiches rocked boats and broke moorings (EBERHART-PHILLIPS *et al.* 2003; CASSIDY and ROGERS 2004). Local bursts of seismic activity were also

observed far away in volcanic and geothermal areas, especially if lying in the direction of the Denali rupture propagation, e.g., in the Yellowstone area, at a distance of 3100 km (HUSEN *et al.* 2004; MORAN *et al.* 2004).

Several papers describe the surface faulting of the 2002 earthquake (EBERHART-PHILLIPS *et al.* 2003; CRONE *et al.* 2004; HAEUSSLER *et al.* 2004; HAEUSSLER 2009). The slip on the Susitna Glacier thrust fault generated structures ranging from simple folds on a

Table 4

Descriptions of relevant environmental effects induced by the 1805 Molise earthquake

Location	Type	Description	References
Pesche, Miranda and S. Angelo in Grotte	Surface faulting	A very long fracture was surveyed from Miranda, Pesche up to S. Angelo in Grotte. "Especially in the upper mountain from Miranda to S. Angelo in Grotte chasms were open for about a half palm" [one Neapolitan palm was 26.3 cm]	FORTINI (1806)
Guardiaregia	Surface faulting	"Very evident and deep fractures with offsets up to seven palms" (about 150 cm according to ESPOSITO <i>et al.</i> 1987).	BARATTA (1901)
Morcone	Surface faulting and hydrological changes	"flames from the ground...were seen near the inn, where horrible chasms opened over a length of about one-third of a mile, some of which had the ground overthrown at a height exceeding six palms, and of which the width was over three palms and comparable the depth. These fractures now can be seen from far away, because the grass along the crevasses is desiccated as it had been on fire. In one such crevasse I observed a pear tree, that, in that moment [of the earthquake], lost all its unripe fruits, threw many branches to the ground and, of the ones left, many are now desiccated. In the same place the soil was completely disturbed, as it had excavated by innumerable moles. Here a spring increased its flow rate, leaving a slight smell of sulphur. A new spring gushed out from the ground..."	CAPOZZI (1834)
Bojano	Karst collapses	The day after the 26 July event, two chasms opened within the Matese Mts. at about a half the slope of Bojano	BARATTA (1901)
Cantalupo	Liquefaction	Several contemporary eye-witnesses documented a liquefaction characterized by sand-volcanoes in the surficial fluvio-lacustrine deposits near the Cantalupo village	PEPE (1806)
S. Giorgio La Molara	Landslide	Along the Tammaro river up to the Molini of Cardinale Ruffo, remarkable vertical as well as horizontal fissures were seen in an area 1922 steps long and about 800 steps wide) [one Neapolitan step, "passo", was ca. 1.9 m]. The topographic surface appeared corrugated and uplifted of about 15 palms; in particular, the poplar tree plantations and a road were uplifted and shifted for 13–20 palms...The Tammaro river was deviated as the original river bed had raised about 50 palms as a consequence of this uplift...	PEPE (1806)
Acquaviva di Isernia	Landslide	"A forest about 20 miles wide was devastated. The ground failed and trees were eradicated"	BARATTA (1901)
Bojano	Emergence of new springs, turbidity, chemical variation	The day before the main shock, some springs located near Bojano were anomalously turbid and hot. Four days later, three large water rivers flooded very quickly the surrounding cultivated fields. The anomaly in water discharge persisted for about 20 days. A new spring opened at Bojano and it is still flowing	POLI (1805) and PEPE (1806)

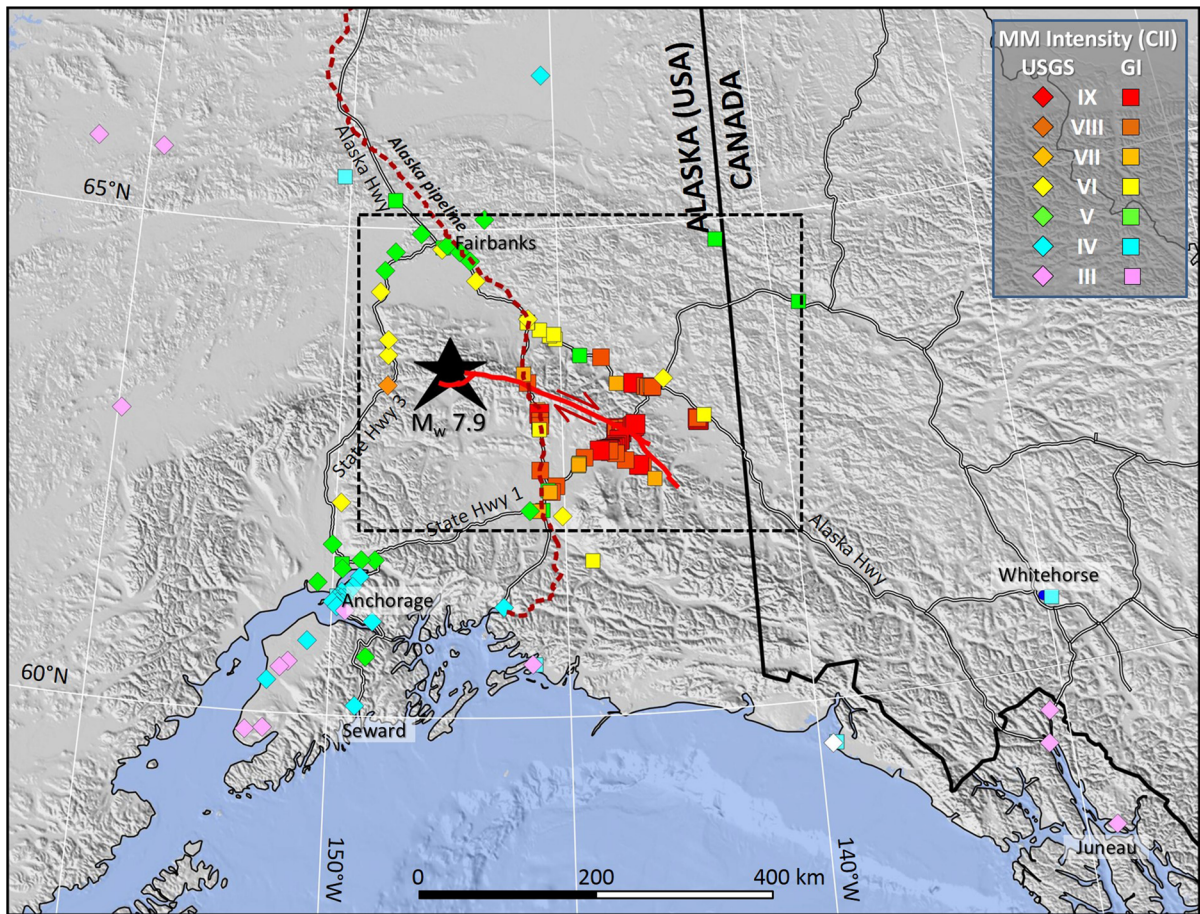


Figure 8

2002 Denali earthquake: Community Internet Intensity (CII) and GI (Geophysical Institute, University of Alaska Fairbanks) intensity distribution based on the report materials (MARTIROSYAN 2004). *Star* indicates the instrumental epicenter. The fault ruptures are plotted, simplified, according to EBERHART-PHILLIPS *et al.* (2003). The *box* encloses the epicentral area (Fig. 9)

single trace to complex thrust-fault ruptures and pressure ridges on multiple, sinuous strands, in a deformation zone locally wider than 1 km. A maximum vertical displacement of 5.4 m on the south-directed main thrust was measured. The principal surface break occurred along 226 km of the Denali fault, with average right-lateral offsets of 4.5–5.1 m and a maximum offset of 8.8 m near its eastern end. Finally, dextral slip averaging 1.6–1.8 m transferred southeastward onto the Totschunda fault for another 66 km.

The secondary geological effects of the 2002 Denali earthquake were mostly landslides, liquefaction and ground cracks (Fig. 9; EBERHART-PHILLIPS *et al.* 2003; Harp *et al.* 2003; HANSEN and

RATCHKOVSKI 2004; JIBSON *et al.* 2004, 2006). Despite the thousands of landslides that were triggered, primarily rock falls, rock slides and rock avalanches, ranging in volume from a few cubic meters to tens of millions of cubic meters (i.e., the rock avalanches that covered much of the McGinnis Glacier), JIBSON *et al.* (2006) have estimated them to be far less than expected for an earthquake of this magnitude and unusually concentrated in only a narrow zone about 30 km wide, straddling the fault-rupture zone over its entire length. The overall affected area of 10,000 km² was significantly smaller than that triggered by other earthquakes of comparable magnitude (HARP *et al.* 2003, and references therein). To explain this, JIBSON *et al.* (2006) suggest a deficit in high-frequency

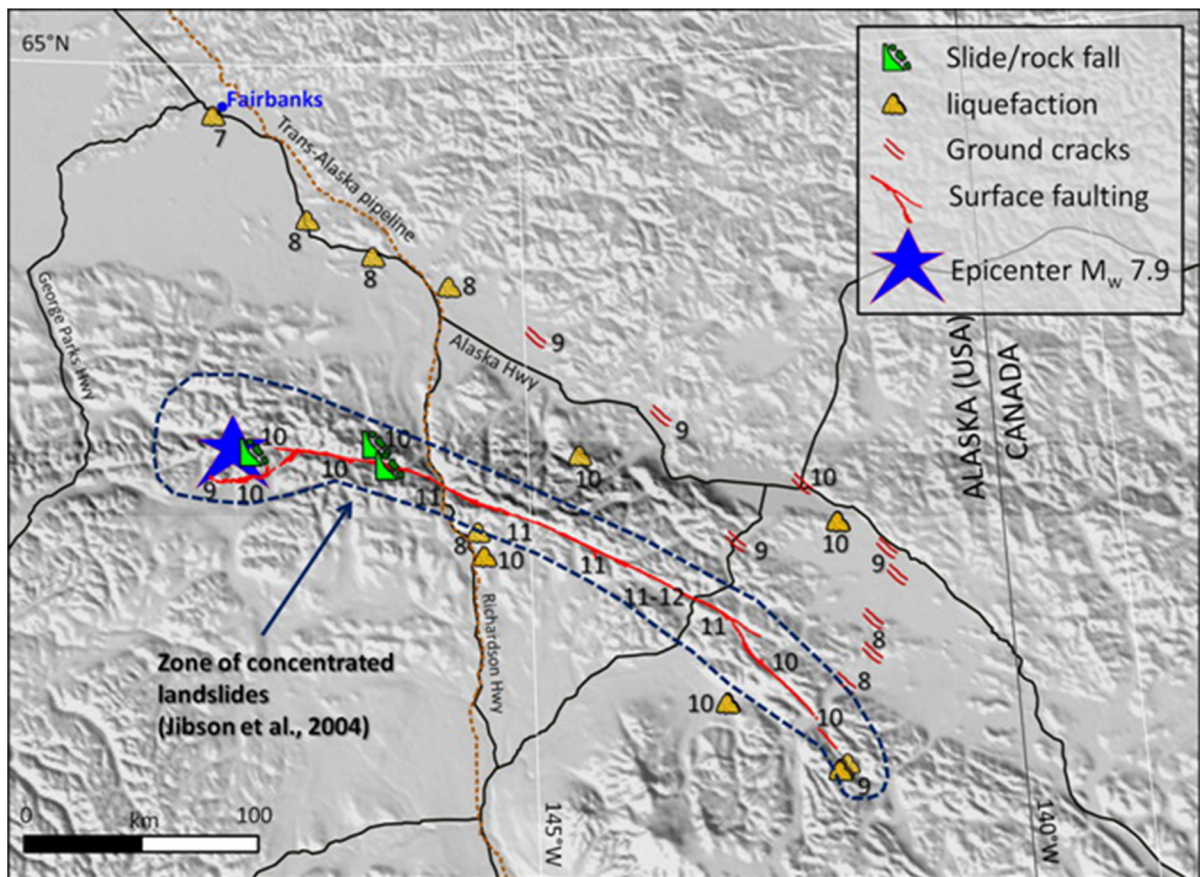


Figure 9

2002 Denali earthquake: distribution of geological effects based on survey data from authors cited in text. The fault ruptures are plotted, simplified, according to EBERHART-PHILLIPS *et al.* (2003)

shaking, with the highest accelerations being confined to the vicinity of the fault zone.

Liquefaction features were observed over a much greater distance, up to 120 km away from the rupture zone. The liquefaction was more extensive and severe to the east, near the third sub-event, on the Holocene alluvial deposits of the Robertson, Slana, Tok, Chisana, Nabesna and Tanana Rivers (EBERHART-PHILLIPS *et al.* 2003; KAYEN *et al.* 2004). Apparently, according to the latter authors, the minimum shaking levels and duration requirements for liquefaction were reached more extensively than those needed to trigger rock falls and rock slides. Actually, the third sub-event had a longer duration and period of shaking than the previous two (HARP *et al.* 2003; KAYEN *et al.* 2004; JIBSON *et al.* 2006). However, also the

stabilizing effect of permafrost may have contributed to reducing the number of mass movements. Moreover, the region surrounding the high peaks of the Alaska Range displays a rather smoother morphology with wide alluvial valleys hosting peri-glacial liquefaction-prone deposits.

Many hydrological anomalies were reported, such as water waves, water spill from swimming pools, seiches in lakes and rivers, muddy well waters, at distances up to 3500 km across western Canada and in the Seattle basin (CASSIDY and ROGERS 2004; BARBEROPOULOU *et al.* 2006; SIL 2006).

The US Geological Survey carried out an indirect macroseismic survey (Community Internet Intensity, CII), later expanded by the University of Alaska Fairbanks (MARTIROSYAN 2004). The combined dataset

contains intensities for more than 155 inhabited locations, 29 of which reported a maximum intensity MM IX. Of these, 28 are located in the eastern part of the ruptured fault, with an average distance from the fault of 27 km (MARTIROSYAN 2004). Most of the reported intensity data come from localities very far (10–100 km) from the fault, and more than 70 % of them are V MMI or less. Their spatial distribution is strongly inhomogeneous, reflecting the sparse population. The USGS has also produced a Shakemap of the event, merging ground motion and macroseismic data (http://earthquake.usgs.gov/earthquakes/eqinthenews/2002/uslbb1/images/AK_mmi_new.jpg) that shows instrumental intensities of at least IX, especially in the central and eastern sections of the rupture zone.

The application of the ESI scale to the diagnostic EEEs reported in the papers above provides intensities between VII and XII for 131 sites (Fig. 10). These intensities are based on evidence of surface faulting (primary effects), slope movements, liquefaction and ground rupture features (secondary effects). Based on the maximum horizontal slip of 8.8 m and the total surface rupture length of 330 km, the maximum ESI scale intensity would be XII. The spatial distribution of secondary effects (landslides and liquefactions), with a total affected area of at least 30,000 km², suggests epicentral intensity XI. Considering only mass movements, the ESI would range between X and XI (Table 3). Such contrasting values might be justified by the multiple rupture and widespread sediments particularly susceptible to liquefaction. As a whole, intensity XI appears most reasonable. The distribution and characteristics of EEEs locates the macroseismic epicenter west of Mentasta, broadly ESE of the instrumental epicenter and near the third sub-event (Fig. 10).

5. Discussion

The three case studies presented in the previous chapter, together with Table 2, help underline the efficacy of environmental effects for improving the evaluation of earthquake size. The maximum intensity of the 1957 Muya earthquake, defined on the basis of its effects on man-made structures is two degrees less than the most reasonable epicentral

intensity, simply because the town nearest to the epicenter is 50 km away. The same holds true for the much more recent 2002 Denali earthquake.

Sprawling infrastructure is not limited to urbanized areas: extensive transportation, water channels and pipeline networks run across the countryside, as well as high-hazard installations such as dams, chemical, nuclear power and Liquefied Natural Gas (LNG) plants. These facilities need be evaluated for geological hazard, and the ESI scale provides a basis for achieving this task. It allows, in a simple and effective manner, the building of scenarios for given intensity values of potential geohazards that an area is liable to face, considering solely its geomorphological and soil characteristics. Practical applicants might be structural designers, regulators, civil protection agencies and administrators, also for a more effective public communication. Even insurance companies may benefit from a comprehensive representation of the seismic hazard at a site, inclusive of geohazards. This remains valid even when dealing with critical facilities, where the most up-to-date and sophisticated methods of SHA are generally applied.

The 1805 Molise earthquake demonstrates that even when surface ruptures are not positively recognized in historical documents, the total area affected by secondary environmental effects can yield a quite accurate assessment of epicentral intensity. This is inferred from the good match of independent epicentral intensity assessments based on primary and secondary environmental effects. At the same time, this case proves the compatibility of the ESI scale with traditional macroseismic scales, where detailed and complete information on earthquake impact on buildings in the epicentral area is available.

Although it has been satisfactorily applied so far, it should be borne in mind that the ESI scale is still a novel tool. Some fine-tuning might prove useful in the future, based on the experience being gained by its application to more cases. In particular, intensity estimates based on primary effects, i.e., SRL or displacement, are a crucial aspect, not considered, for example, in the MMI-derived scale used in New Zealand (HANCOX *et al.* 2002; DOWRICK *et al.* 2008), which instead takes advantage of the shaking-related effects such as mass movements, liquefaction and

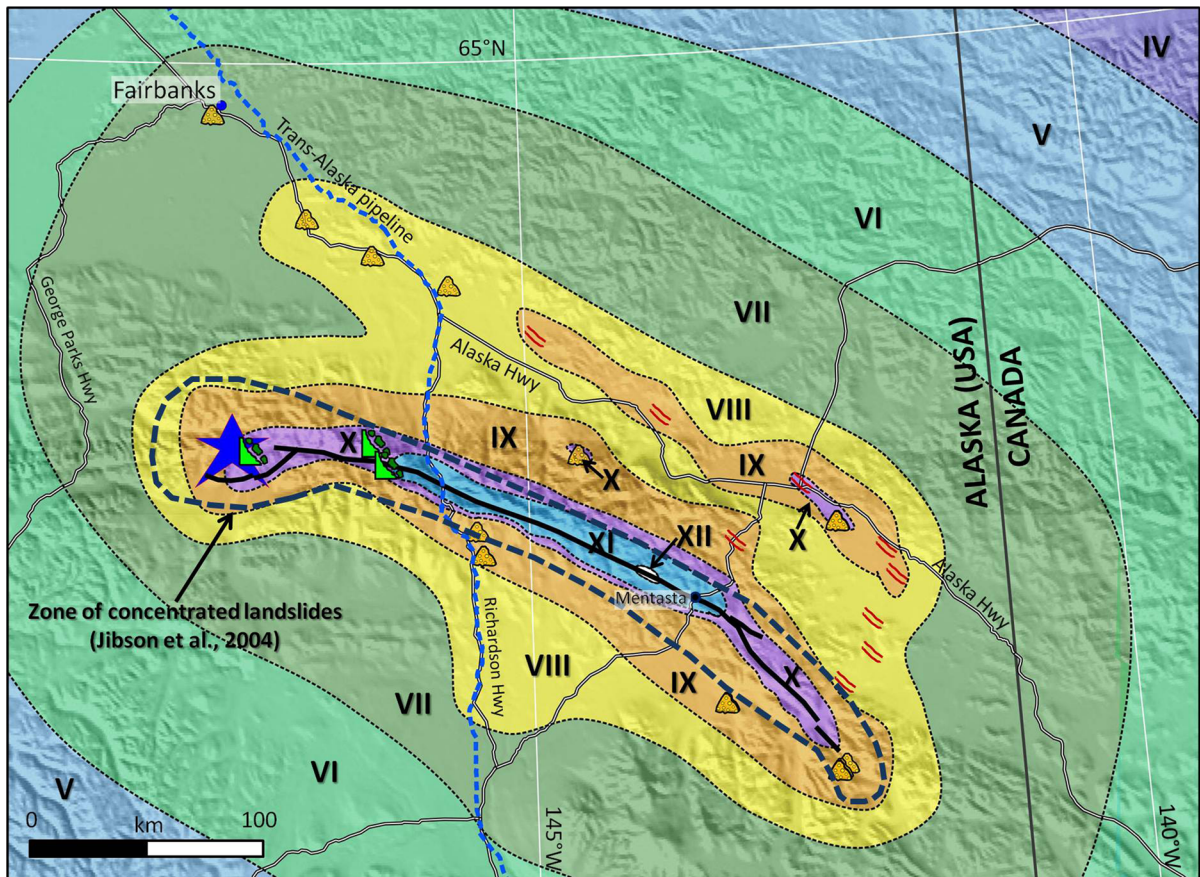


Figure 10

2002 Denali earthquake: intensity field based on CII and ESI intensities. For *symbols*, see legend in Fig. 9. The assessed epicentral (I_0) ESI intensity is XI, based on the amount of slip

other ground damage effects. Large fluctuations in the faulting parameters are commonly observed when compared to magnitude (STIRLING *et al.* 2013, and references therein). The causes are manifold: depth, kinematics and multiple ruptures. The same happens with intensity; therefore, the boundary values given in Table 3 provide a reference frame that must be accompanied by a careful consideration of regional features, such as other rupturing events in the same region, thickness of the seismogenic layer and regional stress-strain state. Possibly, also a characteristic stress-drop may play a role, but there is no general consensus about what it can actually be. For instance, the anomalously short SRL observed for the $M_s = 7.5$ Muya, 1957, earthquake (25 km) is in agreement with all reports of coseismic surface

rupture lengths in the Baikal region, which never exceed 45 km (e.g., TATEVOSSIAN *et al.* 2010). This suggests that such a feature is “characteristic” for the region, driven by a high stress-drop or by an unusually deep seismogenic layer, limiting the portion of the source rupture emerging at surface. Also, the complexity of the rupture process, with nearly pure strike-slip at depth, revealed by focal mechanisms and substantial vertical components of deformation at the surface, points out the need for a careful interpretation of paleo-earthquake data obtained in situ, in light of the regional geodynamics.

In developing the ESI scale, it has always been considered that realistic seismic hazard assessment must be based on a sufficiently wide time-window of earthquake history. Historical accounts of geological

effects commonly inform on secondary effects, such as ground cracks, liquefaction and landslide phenomena, but may also include indications on fault displacement, sometimes even rupture lengths. In addition, erosion or trenching can expose paleoseismic evidence, in the form of time-constrained fault displacements and other geological features, especially filled cracks and liquefaction. Not all EEEs have the same weight in the intensity assessment. Each type of effect depends on some specific parameters, sometimes regional (primary effects), sometimes very local (secondary effects), like morphology, stratigraphy, water table depth and saturation. Some EEEs appear to start from a degree threshold, but subsequently do not allow precise degrees to be defined; others perform better to assess intensities, but always in a statistical sense. There are no clear steps in the number and size of most EEEs between one degree and the next: *Natura non facit saltus*. In general, the more the available EEEs in terms of number and types, the better the intensity estimate. Despite the fact that a single piece of evidence (or several at the same site) may not provide a precise indication of the magnitude of the causative event, it may still represent a key information to confirm the indications deriving from instrumental data or active tectonics studies. Moreover, the size or simply the presence of an EEE does allow a minimum intensity to be assessed, similarly to what is commonly applied in paleoseismology to derive a minimum magnitude threshold. This minimum threshold and the time interval between independent faulting/shaking events can have a strong impact on seismic hazard assessment. In the ESI scale, the uncertainties regarding the value, in terms of earthquake characterization, to be attributed to a local, often single, evidence of faulting, liquefaction or earthquake-triggered mass movement are somehow incorporated in the discrete nature of intensity degrees, which are defined by large boundary values.

With more and more strong-motion recordings made available, attenuation relationships have proliferated based on moment magnitude as the most representative parameter of the source. At the same time, seismologists endeavor to understand the

phenomena involved in source rupturing and propagation, but rarely are their insights taken into account in the design of facilities. Their studies of major recent earthquakes show that the source is complex, and parameters such as rupture length and stress drop, directly linked to slip on the fault plane, are extremely important for source characterization (e.g., MOHAMMADIOUN and SERVA 2001). Stress drop, a parameter linked to maximum acceleration, is strongly variable from one seismotectonic region to another, or even from one fault or seismogenic source to another (e.g., FRY *et al.* 2010). Moreover, the commonly applied ground motion attenuation relationships quite often reveal considerable discrepancies between predicted values and actual data (e.g., SØRENSEN *et al.* 2009). All this calls for a reasonably simple tool to calibrate earthquake size in a straightforward manner from observations of its impact, to be as independent as possible of constraints imposed by models and assumptions.

Macroseismic intensity scales were conceived to determine the size of an earthquake by noting the effects it had caused. However, intensity assessment can be biased by the varying levels of vulnerability displayed by man-made environment. The advantage in founding an intensity scale on geological effects is the opportunity it provides to counterbalance the unavoidable inconsistencies caused by such variable vulnerability. Also, the natural environment is characterized by a varying level of vulnerability. Ground vibratory characteristics affect both secondary geological phenomena and artificial structures. However, the natural environment is more stable on the long-term scale: although ephemeral, it is capable of conserving many EEEs, compared to the man-made environment, being, therefore, able to retain the record of earthquake traces much longer than man-made structures. In fact, damaging effects on the latter strongly depend not only on foundation soil, but also on materials, design and foundation type, which undergo rapid changes, especially in the modern construction industry. This presents an obstacle to a sound comparison of present and past damage. Figure 11 shows examples of this fact, based on the epicentral areas of three large recent earthquakes.



Figure 11

◀ *Top* Photograph shot from a helicopter in the epicentral zone of the 1957 Muya earthquake in 2005, i.e., 48 years after it occurred. The fault trace is still clearly visible, and anyone today can verify its parameters. *Middle* Google Earth image captured in 2010 of the epicentral area of the 1988 Spitak, Armenia, earthquake (22 years after). The two villages in the image were totally destroyed, and intensity 10 was assessed there. Today, it is no longer possible to check any damage-related feature, because the villages have been rebuilt and repaired. *Bottom* The same is true, for opposite reasons, in the epicentral area of the 1995 Neftegorsk earthquake in northern Sakhalin Island, as evident in the Google Earth image of 2010 (15 years after the event). Only a portion of the portrayed building compound collapsed, and intensity 8–9 was assessed for the town at that time. But Neftegorsk was completely abandoned, and this was the reason for further heavy destruction. If someone were to address the 1988 Spitak and the 1995 Neftegorsk earthquakes today, the wrong impression would be that Neftegorsk suffered much heavier damage than the villages in the Spitak epicentral area

contribution of environmental effects is ignored. Table 2 demonstrates this is a generalized problem of worldwide proportions. The case studies presented earlier have served to substantiate this conclusion.

When the epicentral area is located in a densely populated region and detailed information on building damage is available, the ESI scale is to be used in conjunction with one of the “traditional” scales (MSK, MM, EMS). In fact, it must always be borne in mind that intensity in a specific locality results from an informed assessment based on three categories of effects: on human, infrastructures (built environment) and natural environment. Only in such a case does the ESI, which has been developed from the MMI and MSK scales, provide an intensity assessment that is consistent with, and complements the results of, the other scales.

The use of EEEs offers the possibility of comparing earthquake intensities worldwide. In fact, EEEs are uninfluenced by cultural and technological aspects, which may differ significantly from region to region. Moreover, earthquake-prone areas can be located in sparsely or even completely unpopulated regions, where only the effects on the natural environment might be observable. In such a case, ESI becomes the only tool able to calibrate earthquake intensity. The same holds true for events with macroseismic intensity of X and above, where, with most structures being ruined, all the damage-based

6. Conclusions

The main goal of this paper was to introduce the ESI intensity scale, based on environmental effects of earthquakes (EEEs), to the widest possible audience. The key message is that, despite the advent of magnitude, earthquake intensity remains a significant seismic parameter for reliable SHA, especially when EEEs are properly taken into account. In fact, this study shows that epicentral intensity may be underestimated by two or even more degrees if the

intensities tend to saturate. Thus, any assessment based on such damage is biased. Conversely, the size of some EEEs continues to be proportional to the intensity of the earthquake.

It is important to bear in mind that the natural environment may have a much longer memory than the built one. As the impact of an earthquake on a man-made environment depends on the distribution of urbanized areas, it is difficult to compare two seismic events that occurred in the same area, but at very different times. Conversely, this can be achieved on the basis of documented EEEs. This approach extends the time coverage of earthquake catalogues to prehistoric times. Local evidence of surface faulting and the size of secondary effects (i.e., liquefaction effects, landslide-dammed lakes, etc.) pertaining to prehistoric events can be evaluated via detailed paleoseismological investigations in natural or artificial exposures. Thus, the ESI scale allows intensity to be estimated also for paleo-earthquakes.

The ESI scale provides a very convenient guideline for the survey of EEEs in earthquake-stricken areas, ensuring their complete and homogeneous analysis. Its application, continuously improving the EEE catalogue, would consequently also improve the correlations cited above relating magnitude to surface faulting or other geological parameters, which are significantly affected by the inhomogeneity of available data, rarely documented so far with the same criteria and quality.

In conclusion, the factoring in of the geological and geomorphological effects of earthquakes allows the most comprehensive earthquake risk scenario to be built, a crucial need for all stakeholders, especially designers, geotechnical engineers, hazard analysts, regulators, civil protection agencies and insurers, as well as the general population.

Acknowledgments

R. E. Tatevossian was partly funded under RFBR Grant 10-05-00126 and partly by the Cariplo Foundation. G. Hancox has provided valuable criticisms and suggestions that have helped us to greatly improve an earlier version of the manuscript.

Appendix: List of Papers Focusing on the Application of the ESI Scale

FOKAEFS and PAPADOPOULOS (2007), GUERRIERI *et al.* (2007), LALINDE and SANCHEZ (2007), PAPATHANASSIOU *et al.* (2007), PAPATHANASSIOU and PAVLIDES (2007), PORFIDO *et al.* (2007), SERVA *et al.* (2007), TATEVOSSIAN (2007), GUERRIERI *et al.* (2008), SILVA *et al.* (2008), SINTUBIN and STEWART (2008), ZAMUDIO (2008), TATEVOSSIAN *et al.* (2009), ALI *et al.* (2009), MICHETTI *et al.* (2009), MOSQUERA-MACHADO *et al.* (2009), OTA *et al.* (2009), PAPANIKOLAOU *et al.* (2009), BERZHINSKII *et al.* (2010), LEKKAS (2010), PAPANIKOLAOU (2011), GOSAR (2012), FOUNTOULIS and MAVROULIS (2013), MAVROULIS *et al.* (2013), SILVA *et al.* (2013), VELÁZQUEZ-BUCIO *et al.* (2013), BASHIR *et al.* (2014), PAPATHANASSIOU *et al.* (2014), COMERCI *et al.* (2015), PORFIDO *et al.* (2015).

REFERENCES

- AAGAARD, B.T., ANDERSON, G., and HUDNUT, K.W. (2004), *Dynamic rupture modeling of the transition from thrust to strike-slip motion in the 2002 Denali Fault earthquake, Alaska*, Bull. Seism. Soc. Am. 94, S190–S201.
- ABE, K., *Moments and magnitudes of earthquakes, in Global Earth Physics: A Handbook of Physical Constants (ed. Ahrens J.)* (American Geophysical Union, Washington, DC, 1995) 1, pp. 206–213.
- ALI, Z., QAISAR, M., MAHMOOD, T., SHAH, M.A., IQBAL, T., SERVA, L., MICHETTI, A.M., and BURTON, P.W. (2009), *The Muzaffarabad, Pakistan, earthquake of 8 October 2005: Surface faulting, environmental effects and macroseismic intensity*, Geol. Soc. London Spec. Publ. 316, 155–172. doi:10.1144/SP316.9.
- AMBRASEYS, N.N. (1969), Maximum intensity of ground movements caused by faulting, 4th World Conf. Earthquake Eng., Santiago, Chile, 154–171.
- AMBRASEYS, N.N. (1985), *Magnitude assessment of north-western European earthquakes*, J. Earthq. Eng. Struct. Dyn. 13, 307–320.
- ATWATER, B., NELSON, A.R., CLAGUE, J.J., CARVER, G.A., YAMAGUCHI, K., BOBROWSKY, P.T., BOURGEOIS, J., DARIENZO, M.E., GRANT, W.C., HEMPHILL-HALEY, E., KELSEY, H.K., JACOBY, G.C., NISHENKO, S.P., PALMER, S.P., PETERSON, C.D., and REINHART, M.A. (1995), *Summary of coastal geologic evidence for past great earthquakes at the Cascadia Subduction Zone*, Earthquake Spectra 11 (1), 1–18.
- BALAKINA, L.M., VVEDENSKAYA, A.V., GOLUBAVE, N.V., MISHARINA, L.A., and SHIROKOVA, E.I. (1972), The stress Earth field and earthquake mechanisms—Results of studies on International geophysical projects, Seismology 8, M. Nauka, 192 p. (in Russian).
- BANERJEE, P., POLLITZ, F., NAGARAJAN, B., and BURGMANN, R. (2007), *Coseismic Slip Distributions of the 26 December 2004*

- Sumatra–Andaman and 28 March 2005 Nias Earthquakes from GPS Static Offsets*, Bull. Seism. Soc. Am. 97 (1A), S86–S102. doi:10.1785/0120050609.
- BARATTA, M., *I terremoti d'Italia. Saggio di storia, geografia e bibliografia sismica italiana*. (Arnaldo Forni Editore, Torino 1901).
- BARBEROPOULOU, A., QAMAR, A., PRATT, T.L., and STEELE, W.P. (2006), *Long-period effects of the Denali earthquake on water bodies in the Puget lowland: observations and modeling*, Bull. Seism. Soc. Am. 96, 519–535.
- BASHIR, A., HAMID, S., and AKHTAR, A. (2014), *Macroseismic intensity assessment of 1885 Baramulla Earthquake of north-western Kashmir Himalaya, using the Environmental Seismic Intensity scale (ESI 2007)*, Quaternary International 321, 59–64.
- BILHAM, R., ENGDahl, R., FELDL, N., and SATYABALA, S.P. (2005), *Partial and complete rupture of the Indo-Andaman plate boundary 1847–2004*, Seism. Res. Lett. 76, 299–311.
- BLUMETTI, A.M., CACIAGLI, M., DI BUCCI, D., GUERRIERI, L., MICHETTI, A.M., and NASO, G. (2000), *Evidenze di fagliazione superficiale olocenica nel bacino di Bojano (Molise)*, In Proceedings 19th CNR-GNGTS Congress (Rome 2000) pp. 12–15.
- BRAZEE, R.J., and CLOUD, W.K. (1960), *United States earthquakes 1958*, U.S. Coast and Geodetic Survey, 76 p.
- BERZHINSKII, YU.A., ORDYNSKAYA, A.P., GLADKOV, A.S., LUNINA, O.V., BERZHINSKAYA, L.P., RADZIMINOVICH, N.A., RADZIMINOVICH, YA.B., IMAYEV, V.S., CHIPIZUBOV, A.V., and SMEKALIN, O.P. (2010), *Application of the ESI_2007 Scale for Estimating the Intensity of the Kultuk Earthquake, August 27, 2008 (South Baikal)*, Seismic Instruments 46 (4), 307–324.
- CAMPILLO, M., GARIEL, J.C., AKI, K., and SANCHEZ-SESMA, F.J. (1989), *Destructive strong ground motion in Mexico City: Source, path, and site effects during great 1985 Michoacán earthquake*, Bull. Seism. Soc. Am. 79, 1718–1735.
- CAPOZZI, G. (1834), *Memoria sul tremuoto avvenuto nel Contado di Molise nella sera del 26 luglio dell'anno 1805* (Stamperia del Sacro Seminario, Benevento 1834).
- CAPUTO, M., and FAITA, G. (1984), *Primo catalogo dei maremoti delle coste italiane*, Mem. Accad. Naz. Lincei 17 (7), 1–144.
- CASSIDY, J.F., and ROGERS, G.C. (2004), *The Mw 7.9 Denali Fault earthquake of 3 November 2002: Felt reports and unusual effects across Western Canada*, Bull. Seism. Soc. Am. 94, S53–S57.
- CASTILLA, R.A., and AUDEMARD, F. (2007), *Sand blows as a potential tool for magnitude estimation of pre-instrumental earthquakes*, Journal of Seismology 11, 473–487.
- CHAVEZ-GARCIA, F.J., and BARD, P.-Y. (1994), *Site effects in Mexico City eight years after the September 1985 Michoacan earthquakes*, Soil Dynamics and Earthquake Engineering 13, 229–247.
- CHLIEH, M., AVOUAC, J.P., HJORLEIFSDOTTIR, V., SONG, T.A., JI, C., SIEH, K., SLADEN, A., HEBERT, H., PRAWIRODIRDJO, L., BOCK, Y., and GALETZKA J. (2007), *Coseismic Slip and Afterslip of the Great Mw 9.15 Sumatra–Andaman Earthquake of 2004*, Bull. Seism. Soc. Am. 97 (1A), S152–S173.
- COMERCI, V., *Modified Mercalli (MM) scale*, In *Encyclopedia of Natural Hazards* (ed. Bobrowsky P.T.) (Springer Science Business Media B.V., Dordrecht 2013) pp. 683–686.
- COMERCI, V., BLUMETTI, A.M., BRUSTIA, E., DI MANNA, P., GUERRIERI, L., LUCARINI, M., and VITTORI, E., (2013) *Landslides Induced by the 1908 Southern Calabria–Messina Earthquake (Southern Italy)*, In *Landslides Science and Practice, vol 5: complex environment* (ed. Margottini C., Canuti P., and Sassa K.) (Springer, Heidelberg New York Dordrecht London, 2013) pp. 261–267.
- COMERCI, V., VITTORI, E., BLUMETTI, A.M., BRUSTIA, E., DI MANNA, P., GUERRIERI, L., LUCARINI, M., and SERVA, L. (2015), *Environmental effects of the December 28, 1908, Southern Calabria–Messina (Southern Italy) earthquake*, Nat. Hazards 76 (3), 1849–1891. doi:10.1007/s11069-014-1573-x.
- CRONE, A.J., PERSONIUS, S.F., CRAW, P.A., HAEUSSLER, P.J., and STAFF, L.A. (2004), *The Susitna Glacier Thrust Fault: Characteristics of Surface Ruptures on the Fault that Initiated the 2002 Denali Fault Earthquake*, Bull. Seism. Soc. Am. 94, S5–S22.
- DENGLER, L.A., and MCPHERSON, R. (1993), *The 17 August 1991 Honeydew earthquake: a case for revising the Modified Mercalli scale in sparsely populated areas*, Bull. Seism. Soc. Am. 83, 1081–1094.
- DELGADO J., FONSECA MARQUES, F.S., and VAZ, T. (2013), *Seismic-induced landslides in Spain and Portugal*, In *Geología y Arqueología de Terremotos (Geology and Archaeology of Earthquakes)* (ed. Silva P.G., and Huerta P.), Cuaternario & Geomorfología, Spanish Journal of Quaternary and Geomorphology 27 (3–4), 21–35.
- DÉVERCHÈRE, J., PETIT, C., GILEVA, N., RADZIMINOVITCH, N., MELNIKOVA, V., and SAN'KOV, V. (2001), *Depth distribution of earthquakes in the Baikal Rift System and its implications for the rheology of the lithosphere*, Geophys. J. Int. 146, 713–730.
- DI MANNA, P., GUERRIERI, L., PICCARDI, L., VITTORI, E., CASTALDINI, D., BERLUSCONI, A., BONADEO, L., COMERCI, V., FERRARIO, F., GAMBILLARA, R., LIVIO, F., LUCARINI, M., and MICHETTI, A.M. (2013), *Ground effects induced by the 2012 seismic sequence in Emilia: implications for seismic hazard assessment in the Po Plain*, Annals of Geophysics 55 (4), 697–703.
- DOSER, D.I. (1991), *Faulting within the eastern Baikal rift as characterized by earthquake studies*, Tectonophysics 197, 109–139.
- DOWRICK, D.J., HANCOX, G.T., PERRIN, N.D., and DELLOW, G.D. (2008), *The Modified Mercalli Intensity Scale—Revisions arising from New Zealand experience*. Bulletin of the New Zealand Society for Earthquake Engineering, 41(3), 193–205.
- EBERHARD, M.O., BALDRIDGE, S., MARSHALL, J., MOONEY, W., and RIX, G.J. (2010), *The Mw 7.0 Haiti Earthquake of January 12, 2010: USGS/EERI Advance Reconnaissance Team*, USGS Open-File Report 2010–1048, pp. 58.
- EBERHART-PHILLIPS, D., HAEUSSLER, P.J., FREYMUELLER, J.T., FRANKEL, A.D., RUBIN, C.M., CRAW, P., RATCHKOVSKI, N.A., ANDERSON, G., CARVER, G.A., CRONE, A.J., DAWSON, T.E., FLETCHER, H., HANSEN, R., HARP, E.L., HARRIS, R.A., HILL, D.P., HREINSDÓTTIR, S., JIBSON, R.W., JONES, L.M., KAYEN, R., KEEFER, D.K., LARSEN, C.F., MORAN, S.C., PERSONIUS, S.F., PLAFKER, G., SHERROD, B., SIEH, K., SITAR, N., and WALLACE, W.K. (2003), *The 2002 Denali Fault Earthquake, Alaska: A Large Magnitude, Slip-Partitioned Event*, Science 300, 1113–1118.
- EERI (2008), *The Wenchuan, Sichuan Province, China, Earthquake of May 12, 2008*. EERI, Special Earthquake Report, October 2008, pp. 12.
- EERI (2011), *The M 6.3 Christchurch, New Zealand, Earthquake of February 22, 2011*. Learning from Earthquakes, EERI, Special Earthquake Report, May 2011, pp. 16.
- EQE Engineering (1990), *The July 16, 1990 Philippines Earthquake*, EQE Engineering, San Francisco, California, pp. 47.
- ESPINOSA, A.F. (1976), *The Guatemalan earthquake of February 4, 1976*, A preliminary Report, Geological Survey Professional Paper 1002.

- ESPOSITO, E., LUONGO, G., MARTURANO, A., and PORFIDO, S. (1987), *Il terremoto di S. Anna del 26 Luglio 1805*, Mem. Soc. Geol. It. 37, 171–191.
- ESPOSITO, E., GARGIULO, A., IACCARINO, G., and PORFIDO, S. (1998), Distribuzione dei fenomeni franosi riattivati dai terremoti dell'Appennino meridionale. Censimento delle frane del terremoto del 1980, Proc. Int. Conv. Prevention of hydrogeological hazards, CNR-IRPI, Torino, I, 409–429.
- ESPOSITO, E., PECE, R., PORFIDO, S., and TRANFAGLIA, G. (2001), *Hydrological anomalies precursory of earthquakes in Southern Apennines (Italy)*, Natural Hazards and Earth System Sciences 1, 137–144.
- ESPOSITO E., GUERRIERI, L., PORFIDO, S., VITTORI, E., BLUMETTI, A.M., COMERCI, V., MICHETTI, A.M., AND SERVA, L., Landslides Induced by Historical and Recent Earthquakes in Central-Southern Apennines (Italy): A Tool for Intensity Assessment and Seismic Hazard, In *Landslides Science and Practice, vol 5: complex environment* (ed. Margottini C., Canuti P., and Sassa K.) (Springer, Heidelberg New York Dordrecht London, 2013) pp. 8–38.
- FOKAEFS, A., and PAPADOPOULOS, G. (2007), *Testing the new INQUA intensity scale in Greek earthquakes*, Quaternary International 173–174, 15–22.
- FORTINI, P., *Delle Cause de' terremoti e loro effetti, danni di quelli sofferti dalla Città d'Isernia fino a quello de' 26 luglio 1805*, (Sardelli, Marinelli, Isernia 1806).
- FOUNTOULIS, I.G., and MAVROULIS, S.D. (2013), *Application of the Environmental Seismic Intensity scale (ESI 2007) and the European Macroseismic Scale (EMS-98) to the Kalamata (SW Peloponnese, Greece) earthquake (Ms = 6.2, September 13, 1986) and correlation with neotectonic structures and active faults*, Annals of Geophysics 56 (6), S0675. doi:10.4401/ag-6237.
- FRANKEL, A. (2004), *Rupture Process of the M 7.9 Denali Fault, Alaska, Earthquake: Subevents, Directivity, and Scaling of High-Frequency Ground Motions*, Bull. Seism. Soc. Am. 94, S234–S255.
- FRITZ H.M., PETROFF, C.M., CATALÀ, P.A., CIENFUEGOS, R., WINCKLER, P., KALLIGERIS, N., WEISS, R., BARRIENTOS, S.E., MENESES, G., VALDERAS-BERMEJO, C., EBELING, C., PAPADOPOULOS, A., CONTRERAS, M., ALMAR, R., DOMINGUEZ, J.C., and SYNOLAKIS, C.E. (2011), *Field Survey of the 27 February 2010 Chile Tsunami*, Pure Appl. Geophys. 168, 1989–2010.
- FRY, B., BANNISTER, S., BEAVAN, J., BLAND, L., BRADLEY, B., COX, S., COUSINS, J., HANCOX, G., HOLDEN, C., JONGENS, R., POWER, W., PRASETYA, G., REYNERS, M., RISTAU, J., ROBINSON, R., SAMSONOV, S., WELCH, N., WILSON, K, GEO.NET TEAM (2010), *The MW 7.6 Dusky Sound Earthquake of 2009: Preliminary Report*. Bull. New Zealand Society for Earthquake Engineering, 43(1), 24–40.
- GALLI, P. (2000), *New empirical relationships between magnitude and distance for liquefaction*, Tectonophysics 324, 169–187.
- GALLI, P., and GALADINI, F. (2003), *Disruptive earthquakes revealed by faulted archaeological relics in Samnium (Molise, southern Italy)*, Geophys. Res. Lett. 30 (5), 1266. doi:10.1029/2002GL016456.
- GALLI, P., CASTENETTO, S., and PERONACE, E. (2012), *The MCS macroseismic survey of the Emilia 2012 earthquakes*, Ann. Geophys. 55 (4). doi:10.4401/ag-6163.
- GIOFFREDO, P., *Storia delle Alpi Marittime*, (manuscript, ASTo, Fondo mss., H.IV.26, 1692).
- GÓMEZ, J.M., BUKCHIN, B., MADARIAGA, R., ROGOZHIN, E. A., and BOGACHKIN, B. (1997), *Rupture process of the 19 August 1992 Susamyr, Kyrgyzstan, earthquake*, Journal of Seismology 1 (3), 219–235.
- GOSAR, A. (2012), *Application of Environmental Seismic Intensity scale (ESI 2007) to Krn Mountains 1998 Mw = 5.6 earthquake (NW Slovenia) with emphasis on rockfalls*, Nat. Hazards Earth Syst. Sci. 12, 1659–1670. doi:10.5194/nhess-12-1659-2012.
- GRAZIANI, L., BERNARDINI, F., CASTELLANO, C., DEL MESE, S., ERCOLANI, E., ROSSI, A., TERTULLIANI, A., and VECCHI, M. (2015), *The 2012 Emilia (Northern Italy) earthquake sequence: an attempt of historical reading*, J. Seismol. 19, 371–387. doi:10.1007/s10950-014-9471-y.
- GRÜNTHAL, G., *European Macroseismic Scale 1998*, (Cahiers du Centre Européen de Géodynamique et de Séismologie, Luxembourg 1998).
- GUERRIERI, L., SCARASCIA MUGNOZZA, G., and VITTORI, E. (1999), *Analisi stratigrafica e geomorfologica della conoide tardoquaternaria di Campochiaro ed implicazioni per la conca di Bojano in Molise*, Il Quaternario 12 (2), 119–129.
- GUERRIERI, L., TATEVOSSIAN, R., VITTORI, E., COMERCI, V., ESPOSITO, E., MICHETTI, A.M., PORFIDO, S., and SERVA, L. (2007), *Earthquake environmental effects (EEE) and intensity assessment: the INQUA scale project*, Boll. Soc. Geol. It. (Ital. J. Geosci.) Special Section “Tectonic Geomorphology” 8ed. Dramis F., Galadini F., Galli P., Vittori E.) 126 (2), 375–386.
- GUERRIERI L., BLUMETTI, A.M., ESPOSITO, E., MICHETTI, A.M., PORFIDO, S., SERVA, L., TONDI, E., and VITTORI, E. (2008), *Capable faulting, environmental effects and seismic landscape in the area affected by the 1997 Umbria-Marche (Central Italy) seismic sequence*, Tectonophysics 476 (1–2), 269–281. doi:10.1016/j.tecto.2008.10.034.
- HAEUSSLER, P.J., SCHWARTZ, D., DAWSON, T., STENNER, H., LIENKAEMPER, J., SHERROD, B., CINTI, F., MONTONE, P., CRAW, P., CRONE, A., and PERSONIUS, S. (2004), *Surface rupture and slip distribution of the Denali and Totschunda faults in the 3 November 2002 M 7.9 earthquake, Alaska*, Bull. Seism. Soc. Am. 94, S25–S52.
- HAEUSSLER, P.J. (2009), *Surface Rupture Map of the 2002 M7.9 Denali Fault Earthquake, Alaska*; Digital Data, USGS, Data Series 422, U.S. Department of the Interior, U.S. Geological Survey.
- HANCOX, G.T., PERRIN, N.D., and DELLOW, G.D. (2002), *Recent studies of historical earthquake-induced landsliding, ground damage, and MM intensity in New Zealand*. Bulletin of the New Zealand Society for Earthquake Engineering, 35(2), 59–95.
- HANCOX, G.T., RIES, W.F., LUKOVIC, B., and PARKER, R.N. (2014), *Landslides and ground damage caused by the Mw 7.1 Inangahua earthquake of 24 May 1968 in northwest South Island, New Zealand*. GNS Science Report 2014/06. pp. 89.
- HANSEN, R.A., and RATCHKOVSKI, N.A. (2004), *Seismological aspects of the 2002 Denali Fault, Alaska, Earthquake*, Earthquake Spectra 20, 555–563.
- HARBITZ, C.B., LØVHOLT, F., PEDERSEN, G., and MASSON, D.G. (2006), *Mechanisms of tsunami generation by submarine landslides: a short review*. Norw. J. Geol. 86, 255–264.
- HARP, E.L., JIBSON, R.W., KAYEN, R.E., KEEFER, D.K., SHERROD, B.S., CARVER, G.A., COLLINS, B.D., MOSS, R.E.S., and SITAR, N. (2003), *Landslides and liquefaction triggered by the M 7.9 Denali Fault earthquake of 3 November 2002*, GSA Today 13 (8), 4–10.

- HARP, E.L., JIBSON, R.W., and DART, R.L. (2013), *The Effect of Complex Fault Rupture on the Distribution of Landslides Triggered by the 12 January 2010, Haiti Earthquake*, *Landslide Science and Practice* 5, 157–161.
- HARTZELL, S. (1980), *Faulting process of the May 17, 1976 Gazli, USSR earthquake*, *Bull. Seism. Soc. Am.* 70, 1715–1736.
- HAYES G.P., BRIGGS, R.W., SLADEN, A., FIELDING, E.J., PRENTICE, C., HUDNUT, K., MANN, P., TAYLOR, F.W., CRONE, A.J., GOLD, R., ITO, T., and SIMONS, M. (2010), *Complex rupture during the 12 January 2010 Haiti earthquake*, *Nature Geosciences*, published online 10 October 2010. doi:10.1038/NGEO977.
- HIRABAYASHI, C.K., ROCKWELL, T.K., WESNOUSKY, S.G., STIRLING, M.W., and SUAREZ-VIDAL, F. (1996), *A neotectonic study of the San Miguel-Vallecitos fault, Baja California, Mexico*, *Bull. Seism. Soc. Am.* 86, 1770–1783.
- HONEGGER, D.G., CARSON, P.A., CLUFF, L.S., CROUSE, C.B., HACKNEY, D.A., HALL, W.J., JOHNSON, E.R., METZ, M.C., MEYER, K.J., NORTON, J.D., NYMAN, D.J., PAGE, R.A., ROACH, C.H., SLEMMONS, D.B., and SORENSON, S.P. (2004), *Performance of the Trans-Alaska Pipeline system*, *Earthquake Spectra* 20 (3), 707–738.
- HSU, Y., BECHOR, N., SEGALL, P., YU, S., KUO, L., and MA, K. (2002), *Rapid afterslip following the 1999 Chi-Chi, Taiwan Earthquake*, *Geophys. Res. Lett.* 29 (16), 4379–4382. doi:10.1029/2002GL014967.
- HUSEN, S., WIEMER, S., and SMITH, R.B. (2004), *Remotely Triggered Seismicity in the Yellowstone National Park Region by the 2002 Mw 7.9 Denali Fault Earthquake, Alaska*, *Bull. Seism. Soc. Am.* 94 (6B), S317–S331.
- ISC (2012), On-line Bulletin, <http://www.isc.ac.uk>, International Seismological Centre, Thatcham, United Kingdom.
- JIBSON, R.W., HARP, E.L., SCHULZ, W., and KEEFER, D.K. (2004), *Landslides Triggered by the 2002 Denali Fault, Alaska, Earthquake and the Inferred Nature of the Strong Shaking*, *Earthquake Spectra* 20, 669–691.
- JIBSON, R.W., HARP, E.L., SCHULZ, W. and KEEFER, D.K. (2006), *Large rock avalanches triggered by the M-7.9 Denali Fault, Alaska, earthquake of 3 November 2002*, *Engineering Geology* 83, 144–160.
- KANAMORI, H. (1977), *The energy release in great earthquakes*, *J. Geophys. Res.* 82, 2981–2987.
- KAYEN, R., THOMPSON, E., MINASIAN, D., MOSS, R.E.S., COLLINS, B.D., SITAR, N., DREGER, D., and CARVERC, G. (2004), *Geotechnical Reconnaissance of the 2002 Denali Fault, Alaska, Earthquake*, *Earthquake Spectra* 20, 639–667.
- KEEFER, D.K. (1984), *Landslides caused by earthquakes*, *Bull. Seism. Soc. Am.* 95, 406–421.
- KIKUCHI, M., and YAMANAKA, Y. (2002), *Source rupture processes of the central Alaska earthquake of Nov. 3, 2002, inferred from teleseismic body waves (+ the 10/23 M6.7 event)*, *EIC Seismological Note* 129.
- KONDORSKAYA, N.V., and SHEBALIN, N.V. (editors) (1982), *New catalog of strong earthquakes in the U.S.S.R. from ancient times through 1977*, report SE-31, NOAA-NGDC, Boulder, USA, pp. 608.
- KURUSHIN, R.A. (1963), *Pleistoseismic region of Muya earthquake (in Russian)*, *Geol. Geofiz.* 5, 122–126.
- KURUSHIN, R.A., and MEL'NIKOVA, V.I., (2008), *Destruction of the Earth's crust during the Muya earthquake in 1957 (M_lh = 7.6)*, *Doklady Earth Sciences* 421 (2), 974–977.
- LALINDE, C.P., and SANCHEZ, J.A. (2007), *Earthquake and environmental effects in Colombia in the last 35 years. INQUA Scale Project*, *Bull. Seism. Soc. Am.* 97 (2), 646–654.
- LEKKAS, E.L. (2010), *The 12 May 2008 Mw 7.9 Wenchuan, China, earthquake: macroseismic intensity assessment using the EMS-98 and ESI 2007 Scales and their correlation with the geological structure*, *Bull. Seism. Soc. Am.* 100 (5B), 2791–2804. doi:10.1785/0120090244.
- LOCATI, M., CAMASSI, R., and STUCCHI, M. (eds.) (2011), *DBMI11, the 2011 version of the Italian Macroseismic Database*. Milano, Bologna, <http://emidius.mi.ingv.it/DBMI11>. doi:10.6092/INGV.IT-DBMI11.
- LOUPEKINA, I.S. (1966), *Earthquake reconnaissance mission: Uganda—the Toro earthquake of 20 March 1966*, UNESCO, Paris.
- MARAMAI, A., BRIZUELA, B., AND GRAZIANI, L. (2014), *The Euro-Mediterranean Tsunami Catalogue*. *Annals Geoph.* 57(4), S0435. doi:10.4401/ag-6437.
- MARTIN, S.S. (2005), *Intensity Distribution from the 2004 M 9.0 Sumatra-Andaman Earthquake*, *Seism. Res. Letters* 76, 321–330.
- MARTIROSYAN, A.H. (2004), *Macroseismic survey of the M 7.9, 2002 Denali fault Earthquake*. Final Technical Report, Geophysical Institute, University of Alaska Fairbanks, pp. 24.
- MAVONGA, T., and DURRHEIM R.J. (2009), *Seismic hazard in the DRC and Western Rift Valley of Africa*, 11th SAGA Biennial Technical Meeting and Exhibition, Swaziland, pp. 66.
- MAVROULIS, S.D., FOUNTOULIS, I.G., SKOURTSOS, E.N., LEKKAS, E., and PAPANIKOLAOU, I.D. (2013), *Seismic intensity assignments for the 2008 Andravida (NW Peloponnese, Greece) strike-slip event (June 8, Mw = 6.4) based on the application of the Environmental Seismic Intensity scale (ESI 2007) and the European Macroseismic scale (EMS-98)*, *Geological structure, active tectonics, earthquake environmental effects and damage pattern*, *Annals of Geophysics* 56 (6), S0681. doi:10.4401/ag-6239.
- MCCALPIN, J.P. (ed.) (2009), *Paleoseismology, 2nd Edition, International Geophysics Series 95*, Elsevier Publishing, 647 p.
- MICHETTI, A.M., ESPOSITO, E., GÜRPNAR, A., MOHAMMADIOUN, B., MOHAMMADIOUN, G., PORFIDO, S., ROGHOZIN, E., SERVA, L., TATEVOSSIAN, R., VITTORI, E., AUDEMARD, F., COMERCI, V., MARCO, S., MCCALPIN, J., and MÖRNER, N.A., (2004) *The INQUA Scale. An innovative approach for assessing earthquake intensities based on seismically-induced ground effects in natural environment*, In *Memorie Descrittive della Carta Geologica d'Italia, Special Volume 67* (ed. Vittori E., and Comerchi V.), (APAT, Rome 2004) pp. 1–118.
- MICHETTI, A.M., ESPOSITO, E., GUERRIERI, L., PORFIDO, S., SERVA, L., TATEVOSSIAN, R., VITTORI, E., AUDEMARD, F., AZUMA, T., CLAGUE, J., COMERCI, V., GÜRPNAR, A., MC CALPIN, J., MOHAMMADIOUN, B., MÖRNER, N.A., OTA, Y., and ROGHOZIN, E., *Intensity Scale ESI 2007*, In *Memorie Descrittive della Carta Geologica d'Italia, Special Volume 74* (ed. Guerrieri L., and Vittori E.), (APAT, Rome 2007) pp. 7–54.
- MICHETTI, A.M., VITTORI, E., BERLUSCONI, A., BLUMETTI, A.M., COMERCI, V., DI MANNA, P., ESPOSITO, E., GUERRIERI, L., LIVIO, F., PORFIDO, S., and SILEO, G. (2009), *Earthquake Ground Effects during Moderate Events: the L'Aquila 2009 Event Case history*, in *Proceedings of the 1st INQUA-IGCP-567 International Workshop on Earthquake Archaeology and Paleoseismology*, Baelo Claudia, Spain (2009) pp. 87–90, ISSN ISBN 978-84-7484-217-3.

- MOHAMMADIOUN, B., and SERVA, L. (2001), *Stress Drop, Slip Type, Earthquake Magnitude and Seismic Hazard*, Bull. Seism. Soc. Am. *91*, 694–707.
- MORAN, S.C., POWER, J.A., STIHLER, S.D., SANCHEZ, J.J., and CAMPAN-AUERBACH, J. (2004), *Earthquake triggering at Alaskan volcanoes following the 3 November 2002 Denali Fault earthquake*, Bull. Seism. Soc. Am. *94*, S300–S309.
- MORI, N., TAKAHASHI, T., YASUDA, T., and YANAGISAWA, H. (2011), *Survey of 2011 Tohoku earthquake tsunami inundation and run-up*, Geophys. Res. Lett. *38*, L00G14. doi:[10.1029/2011GL049210](https://doi.org/10.1029/2011GL049210)
- MOSQUERA-MACHADO, S., LALINDE-PULIDO, C., SALCEDO-HURTADO, E., and MICHETTI, A.M. (2009), *Ground effects of the October 18, 1992, Murindo Earthquake (NW Colombia), using the Environmental Seismic Intensity Scale (ESI 2007) for the assessment of the intensity*, Geol. Soc. London Spec. Publ. *316*, 123–144. doi:[10.1144/SP316.7](https://doi.org/10.1144/SP316.7).
- MUSHKETOV, I.V. (1890), Верненское землетрясение 28 мая (9 июня) 1887 г. // Труды Геологического комитета, X(1), Le tremblement de terre de Verny, 28 Mai (9 Juin) 1887. Mémoires du Comité Géologique X(1).
- MUSSON, R.M.W., GRÜNTAL, G., and STUCCHI, M. (2010), *The comparison of macroseismic intensity scales*, J. Seismol. *14*, 413–428. doi:[10.1007/s10950-009-9172-0](https://doi.org/10.1007/s10950-009-9172-0).
- NIKONOV, A.A., VAKOV, A.V., and VESELOV, I.A. (1983), *Seismotectonics and earthquakes in the convergent zone between the Pamir and the Tien Shan*: Moscow, Nauka 240 (in Russian).
- NISHIMAE, Y. (2004), *Observation of seismic intensity and strong ground motion by Japan Meteorological Agency and local governments in Japan*. J. Japan Ass. For Earthquake Eng., *4* (3), 75–78.
- OTA, Y., AZUMA, T., and LIN, N. (2009), *Application of INQUA Environmental Seismic Intensity Scale to recent earthquakes in Japan and Taiwan*, Geol. Soc. London Spec. Publ. *316*, 55–71.
- OZAWA, S., NISHIMURA, T., SUITO, H., KOBAYASHI, T., TOBITA, M., and IMAKIIE, T. (2011), *Coseismic and postseismic slip of the 2011 magnitude-9 Tohoku-Oki earthquake*, Nature *474*, 373–376.
- PANZA, G.F., VACCARI, F. and CAZZARO, R. (1997), *Correlation between macroseismic Intensities and seismic ground motion parameters*, Annali Geofisica *15*, 1371–1382.
- PAPANIKOLAOU, I.D. (2011), *Uncertainty in intensity assignment and attenuation relationships: How seismic hazard maps can benefit from the implementation of the Environmental Seismic Intensity scale (ESI 2007)*, Quaternary International *242*, 42–51.
- PAPANIKOLAOU I.D., PAPANIKOLAOU, D.I., and LEKKAS, E.L. (2009), *Advances and limitations of the Environmental Seismic Intensity scale (ESI 2007) regarding near-field and farfield effects from recent earthquakes in Greece: implications for the seismic hazard assessment*, In *Paleoseismology: Historical and Prehistorical Records of Earthquake Ground Effects for Seismic Hazard Assessment* (ed. Reicherter K., Michetti A.M., and Silva Barroso P.G.), Geol. Soc. London Spec. Publ. *316*, 11–30.
- PAPATHANASSIOU, G., and PAVLIDES, S. (2007), *Using the INQUA Scale for the Assessment of Intensity: Case Study of the 2003 Lefkada (Ionian Islands), Greece Earthquake*, Quaternary International *173–174*, 4–14.
- PAPATHANASSIOU, G., VALKANIOU, S., and PAVLIDES, S. (2007), *Applying the INQUA Scale to the Sfoaeds 1954, Central Greece, earthquake*, Bull. Geol. Soc. of Greece XXXVII, 1226–1233.
- PAVLIDES, S. and CAPUTO, R. (2004), *Magnitude versus faults' surface parameters: quantitative relationships from the Aegean Region*, Tectonophysics *380*, 159–188.
- PAVLIDES, S., PAPATHANASSIOU, G., VALKANIOU, S., CHATZIPETROS, A., SBORAS, S., and CAPUTO, R. (2013), *Rock-falls and liquefaction related phenomena triggered by the June 8, 2008, Mw = 6.4 earthquake in NW Peloponnesus, Greece*, Annals of Geophysics *56* (6), S0682. doi:[10.4401/ag-5807](https://doi.org/10.4401/ag-5807).
- PEPE, G., *Ragguaglio storico-fisico del terremoto accaduto nel Regno di Napoli la sera del 26 luglio 1805 (Napoli 1806)*.
- POLI, G.S., *Memoria sul terremoto dé 26 luglio del corrente anno 1805 (Napoli 1805)*.
- PORFIDO, S., ESPOSITO, E., MICHETTI, A.M., BLUMETTI, A.M., VITTORI, E., TRANFAGLIA, G., GUERRIERI, L., FERRELLI, L., and SERVA, L. (2002), *Areal distribution of ground effects induced by strong earthquakes in the Southern Apennines (Italy)*, Surveys in Geophysics *23*, 529–562.
- PORFIDO, S., ESPOSITO, E., GUERRIERI, L., VITTORI, E., TRANFAGLIA, G., and PECE, R. (2007), *Seismically induced ground effects of the 1805, 1930 and 1980 earthquakes in the Southern Apennines, Italy*, Ital. J. Geosci. (Boll. Soc. Geol. It.) *126*, 333–346.
- PORFIDO, S., ESPOSITO, E., SACCHI, M., MOLISSO, F., and MAZZOLA, S. (2015), *Impact of Ground Effects for an appropriate mitigation strategy in seismic areas: the example of Guatemala 1976 earthquake*, In: Lollino, G., et al. (Eds.), *Engineering Geology for Society and Territory 2*, 703–708.
- REITER, L., (1990) *Earthquake Hazard Analysis: Issues and Insights* (Columbia University Press, New York 1990).
- RICHTER, C.F. (1935), *An instrumental earthquake magnitude scale*. Bull. Seism. Soc. Am. *25* (1–2), 1–32.
- RICHTER, C.F., (1958) *Elementary Seismology* (Freeman and Company, San Francisco 1958).
- RODRÍGUEZ, C., BOMMER, J., and CHANDLER, R. (1999), *Earthquake-induced landslides: 1980–1997*, Soil Dyn. Earthquake. Eng. *18*, 325–346.
- RUEGG, J.C., OLCAY, M., and LAZO, D. (2001), *Co, post and pre (?) seismic displacements associated with the Mw 8.4 southern Peru earthquake of June 23, 2001, from continuous GPS measurements*, Seism. Res. Letters *72*, 673–678.
- SATAKE, K., FUJII, Y., HARADA, T., and NAMEGAYA, Y. (2013), *Time and slip distribution of coseismic slip of the 2011 Tohoku earthquake as inferred from tsunami waveform data*, Bull. Seism. Soc. Am. *103*, 1473–1492. doi:[10.1785/0120120122](https://doi.org/10.1785/0120120122), 2013.
- SERVA, L. (1994), *The effects on the ground in the intensity scales*, Terra Nova *6*, 414–416.
- SERVA, L., ESPOSITO, E., GUERRIERI, L., PORFIDO, S., VITTORI, E., and COMERCI, V. (2007), *Environmental Effects from some historical earthquakes in Southern Apennines (Italy) and macroseismic intensity assessment. Contribution to INQUA EEE scale project*, Quaternary International *173–174*, 30–44.
- SHEBALIN, N.V. (1972), *Macroseismic data as information on source parameters of large earthquakes*, Physics of the Earth and Planetary Interiors *6*, 316–323.
- SHEBALIN, N.V. (1975), *On seismic intensity evaluation (in Russian)*, Seysmiche skiyeshkalyi metody izmereniya seysmicheskoyo pasnosti (Seismic scales and methods of seismic hazard assessment), 87–109.
- SIL, S. (2006), *Response of Alaskan wells to near and distant large earthquakes*, M.S. Thesis, University of Alaska Fairbanks, pp. 83.

- SILVA, P.G., RODRÍGUEZ PASCUA, M.A., PÉREZ-LÓPEZ, R., BARDAJÍ, T., LARIO, J., ALFARO, P., MARTÍNEZ-DÍAZ, J.J., REICHERTER, K., GIMÉNEZ GARCÍA, J., GINER, J., AZAÑÓN, J.M., GOY, J.L., and ZAZO, C. (2008), *Catalogacion de los efectos geologicos y ambientales de los terremotos en Espana en la Escala ESI 2007 y su aplicacion a los estudios paleosismologicos*, *Geotemas* 6, 1063–1066.
- SILVA, P.G., PÉREZ-LÓPEZ, R., RODRÍGUEZ-PASCUA, M.A., GINER, J.L., HUERTA, P., BARDAJÍ, T., and MARTÍN-GONZÁLEZ, F. (2013), Earthquake Environmental Effects (EEEs) triggered by the 2011 Lorca earthquake (Mw 5.2, Betic Cordillera, SE Spain): Application of the ESI-07 Macroseismic Scale, In Proceedings of the 4th International INQUA Meeting on Paleoseismology, Active Tectonics and Archeoseismology (PATA), 9–14 October 2013, Aachen, Germany, pp. 237–240. ISBN: 978-3-00-042796-1.
- SINTUBIN, M., and STEWART, I. (2008), *A logical methodology for Archaeoseismology: a proof of concept at the archaeological site of Sagalassos, Southwest Turkey*, *Bull. Seism. Soc. Am.* 98, 2209–2230.
- SOKOLOV, V., and WALD, D.J. (2002), *Instrumental Intensity Distribution for the Hector Mine, California, and the Chi-Chi, Taiwan, Earthquakes: Comparison of Two Methods*, *Bull. Seism. Soc. Am.* 92, 2145–2162.
- SOLOENENKO, V.P., TRESKOV, A.A., FLORENISOV, N.A., and PUCHKOV, S.V. (1958), *Muya Earthquake, June 27, 1957 (in Russian)*, *Vopr. Inzh. Seismol.* 1, 29–43.
- SOLOENENKO, V.P. (1965), *Living tectonics in Pleistocene region of Muya earthquake (in Russian)*, *Izv. Akad. Nauk USSR, Ser. Geol.*, 4, 58–70.
- SOLOENENKO, V.P., TRESKOV, A.A., KURUSHINA, R.A., MISHARINA, L.A., PAVLOV, O.V., PSHENNIKOV, K.V., SOLOENENKO, M.A., FOMINA, E.V., and KHLIL'KO, S.D. (1966), *Zhivayatektonika, vulkanyseismichnost' Stanovogonagor'ya (Living Tectonics, Volcanoes and Seismicity of Stanovoi Highland)*, Nauka, Moscow.
- SOLOENENKO, V.P., NIKOLAIEV, V.V., SEMENOV, R.M., DEM'YANOVICH, M.G., KURUSHIN, R.A., KHROMOVSKIKH, V.S., and CHIPUZBOV, A.V. (1985), *Geologiya i seismichnost' zony BAM. Seismologiya i seismicheskoeaionirovanie (Geology and Seismicity of BAM. Seismology and Seismic Regionalization)*, Nauka, Novosibirsk.
- STIRLING, M., RHOADES, D., and BERRYMAN, K. (2002), *Comparison of earthquake scaling relations derived from data of the instrumental and preinstrumental era*, *Bull. Seism. Soc. Am.* 92 (2), 812–830.
- STIRLING, M., GODED, T., BERRYMAN, K., and LITCHFIELD, N. (2013), *Selection of earthquake scaling relationships for seismic hazard analysis*, *Bull. Seism. Soc. Am.* 103 (6), 2993–3011.
- STOVER, C.W., and COFFMAN, J.L. (1993), *Seismicity of the United States, 1568–1989 (Revised)*, U.S. Geological Survey Professional Paper 1527, pp. 418.
- SØRENSEN M.B., STROMEYER, D., and GRÜNTAL G. (2009), *Attenuation of macroseismic intensity: a new relation for the Marmara Sea region, Northwest Turkey*, *Bull. Seism. Soc. Am.* 99 (2A), 538–553.
- TATEVOSSIAN, R.E. (2007), *The Verny, 1887, Earthquake in Central Asia: Application of the INQUA Scale based on Coseismic Environmental Effects. Dark Nature: rapid environmental change and human response*, *Quaternary International* 173–174, 23–29.
- TATEVOSSIAN, R.E., ROGOZHIN, E.A., AREFIEV, S.S., and OVSYUCHENKO, A.N. (2009), *Earthquake intensity assessment based on environmental effects: principles and case studies*, *The Geological Society of London Special Publication* 316, 73–91. doi:10.1144/SP316.5.
- TATEVOSSIAN, R.E., MOKRUSHINA, N.G., OVSYUCHENKO, A.N., and TATEVOSSIAN, T.N. (2010), *Geological and Macroseismic Effects of the Muya, 1957 Earthquake and Paleoearthquakes in Baikal Region*, *Seismic Instruments* 46 (2), 166–191.
- TATEVOSSIAN, R.E. (2011), *On the problem of magnitude calibration of paleo earthquakes*, *Quaternary International* 242, 11–19.
- TAVERA, H., BUFORN, E., BERNAL, I., ANTAYHUA, Y., and VILACAPOMA, L. (2002), *The Arequipa (Peru) earthquake of June 23, 2001*, *Journal of Seismology* 6, 279–283.
- TEN BRINK, U.S., LEE, H.J., GEIST, E.L., and TWICHELL, D.C. (2009), *Assessment of tsunami hazard to the U.S. Atlantic Coast using relationships between submarine landslides and earthquakes*, *Marine Geology* 264, 65–73.
- TINTI, S., and MARAMAI, A. (1996), *Catalogue of tsunamis generated in Italy and in Côte d'Azur, France: a step towards a unified catalogue of tsunamis in Europe*, *Annali Geofisica* 39, 1253–1299.
- VALKANIOTIS, S., GANAS, A., PAPATHANASSIOU, G., PAPANIKOLAOU, M. (2014), *Field observations of geological effects triggered by the January–February 2014 Cephalonia (Ionian Sea, Greece) earthquakes*, *Tectonophysics* 630, 150–157.
- VELÁZQUEZ-BUCIO, M.M., MICHETTI, A.M., BENENTE, L., GROPELLI, G., GARDUÑO-MONROY, V.H., FILONZI, S., RODRÍGUEZ-PASCUA, M.A., PÉREZ-LÓPEZ, R., and CHUNGA, K. (2013), *ESI2007 assessment of paleoseismic features in the Acambay and Ixtlahuaca graben, Mexico: evidence for capability along the Perales Fault*, In Proceedings of the 4th International INQUA Meeting on Paleoseismology, Active Tectonics and Archeoseismology (PATA), 9–14 October 2013, Aachen, Germany, pp. 285–289. ISBN: 978-3-00-042796-1.
- VITTORI, E., DI MANNA, P., BLUMETTI, A.M., COMERCI, V., GUERRIERI, L., ESPOSITO, E., MICHETTI, A.M., PORFIDO, S., PICCARDI, L., ROBERTS, G., BERLUSCONI, A., LIVIO, F., SILEO, G., WILKINSON, M., MCCAFFREY, K.J.W., PHILLIPS, R.J., and COWIE, P.A. (2011), *Surface faulting of the April 6, 2009, Mw 6.3 L'Aquila earthquake in Central Italy*, *Bull. Seism. Soc. Am.* 101, 1507–1530. doi:10.1785/0120100140.
- VON HAKE, C.A., and CLOUD, W.K. (1966), *United States earthquakes 1964*, U.S. Coast and Geodetic Survey, pp. 91.
- VVEDENSKAYA, A.V., and BALAKINA, L.M. (1960), *Stress reconstruction in earthquake sources of the Baikal region and Mongolia: Methods and results*, *Bull. Seismol. Sov. AN SSSR* 10, 73–84.
- WALD, D.J., QUITORIANO, V., HEATON, T.H., and KANAMORI, H. (1999), *Relationships between peak ground acceleration, peak ground velocity, and modified Mercalli intensity in California*, *Earthq. Spectra* 15 (3), 557–564.
- WANG, H., and TAO, X. (2003), *Relationships between moment magnitude and fault parameters: theoretical and semi-empirical relationships*, *Earthquake Eng. Vib.* 2 (2), 201–211.
- WARD, S.N. (2001), *Landslide tsunami*, *J. Geophys. Res.* 106, 11201–11215.
- WELLS, L.D., and COPPERSMITH, J.K. (1994), *New Empirical Relationships among Magnitude, Rupture Length, Rupture Width, Rupture Area, and Surface Displacement*, *Bull. Seism. Soc. Am.* 84, 974–1002.
- WRIGHT, T.J., LU, Z., and WICKS, C. (2004), *Constraining the slip distribution and fault geometry of the Mw 7.9, 3 November 2002,*

- Denali Fault earthquake with Interferometric Synthetic Aperture Radar and Global Positioning System data*, Bull. Seism. Soc. Am. *94*, S175–S189.
- YEATS, S.A., YEATS, R.S., SIEH, K.E., and ALLEN, C.R., *The Geology of Earthquakes* (Oxford University Press, New York 1997).
- ZAMUDIO, J. (2008), New scale of macroseismic intensity-ESI 2007 applied to Peruvian earthquakes, In Proceedings of the 33th International Geological Congress, Oslo, 6–14 August 2008, Session STP02.
- ZECCHI, R. (2004), *The seismicity of Italy in medium and small scale maps*, Boll. AIC *120*, 111–125.

(Received February 3, 2015, revised September 8, 2015, accepted September 13, 2015, Published online October 13, 2015)